

**Material Science and Technology Division**

**Propulsion Materials Program  
Quarterly Progress Report for  
October through December 2008**

**D. R. Johnson  
Technical Project Manager**

**Prepared for  
U.S. Department of Energy  
Assistant Secretary for Energy Efficiency and Renewable Energy  
Office of Vehicle Technologies Program  
VT 05 04 000**

**Prepared by the  
OAK RIDGE NATIONAL LABORATORY  
Oak Ridge, Tennessee 37831-6066  
Managed by  
UT-Battelle, LLC  
for the Department of Energy  
Under contract DE-AC05-00OR22725**

## CONTENTS

### **Project 18516 – Materials for Electric and Hybrid Drive Systems**

*Agreement 16307 – Modeling/Testing of Environmental Effects on PE Devices (ORNL)*

*Agreement 16305 – Materials by Design – Solder Joint Analysis (ORNL)*

*Agreement 16306 – Materials Compatibility of Power Electronics (ORNL)*

### **Project 18517 – Combustion System Materials**

*Agreement 11752 – Advanced Materials Development through Computational Design for HCCI Engine Applications (ORNL)*

### **Project 18518 – Materials for High Efficiency Engines**

*Agreement 16303 – Materials for High Pressure Fuel Injection Systems (ORNL)*

*Agreement 16304 – Materials for Advanced Engine Valve Train (CRADA with Caterpillar) (ORNL)*

*Agreement 13329 – Design Optimization of Piezoceramic Multilayer Actuators for Heavy Duty Diesel Engine Fuel Injectors (ORNL)*

*Agreement 13332 – Friction and Wear Reduction in Diesel Engine Valve Trains (ORNL)*

*Agreement 9089 – NDE Development for ACERT Engine Components (ANL)*

*Agreement 15050 – Materials-enabled High Performance Diesel Engines (CRADA with Caterpillar) (ORNL)*

### **Project 18519 – Materials for Control of Exhaust Gases and Energy Recovery Systems**

*Agreement 9130 - Development of Materials Analysis Tools for Studying SCR Catalysts (CRADA with Cummins) (ORNL)*

*Agreement 10461 - Durability and Reliability of Ceramic Substrates for Diesel Particulate Filters (CRADA with Cummins) (ORNL)*

*Agreement 10635 – Catalysis by First Principles - Can Theoretical Modeling and Experiments Play a Complimentary Role in Catalysis? (ORNL)*

**Project 18865 – Materials by Design**

*Agreement 9105 - Ultra-High Resolution Electron Microscopy for Characterization of Catalyst Microstructures and De-activation Mechanisms (ORNL)*

*Agreement 17895 – Durability of ACERT Engine Components (ORNL)*

*Agreement 14957 – High Temperature Thermoelectrics (CRADA with Marlow) (ORNL)*

*Agreement 16308 – Science Based Approach to Thermoelectric Materials (ORNL)*

## **Agreement 16307: Modeling/Testing of Environmental Effects on PE Devices**

**A. A. Wereszczak, T. P. Kirkland, O. M. Jadaan, and R. Wiles  
Oak Ridge National Laboratory**

### **Objective/Scope**

Understand the complex relationship between environment (temperature, humidity, and vibration) and the performance and reliability of the material constituents within automotive power electronic (PE) devices. There is significant interest in developing more advanced PE devices and systems for transportation applications (e.g., hybrid electric vehicles, plug-in hybrids) that are capable of sustained operation to 200°C. Advances in packaging materials and technology can achieve this but only after their service limitations are better understood via modeling and testing.

### **Technical Highlights**

The work this quarter primarily focused on the strength testing and effective length evaluations of three different mechanical testing configurations designed to specifically promote failure initiation at edges of silicon and silicon carbide chips.

The three test configurations are shown in Fig. 1. They are used to subject the 10x10x0.25 mm silicon and silicon carbide plates to three-point-bending, anticlastic bending, or ring-on-ring bending. Because these chips are so highly polished, the presumption was that edge-located flaws would be more apt to cause fracture than any present surface flaws.

The produced stress distributions for each of the three loading configurations are shown in Fig. 2. The manner in which the effective length for each was determined is shown as well. The resulting effective length as a function of Weibull modulus for each is shown in Fig. 3. The functions shown in Fig. 3 enable strength-size-scaling for the same strength-limiting flaw type.

There are advantages and disadvantages to each method. The three point-bending is the simplest configuration; however, it samples the least amount of edge length for flaws, and if there's differences in the surface condition of both sides of the chip and orientation (which is true for both for the silicon chips and the latter true for the silicon carbide chips), then up to four combinations of test sets need to be generated. The advantage of the anticlastic bending is that it establishes the shown stress profile in Fig. 2 on all eight edges, and therefore, if there's a weakest side among them, then in principal, this test method would exploit that. The disadvantages are the Hertzian contact stresses caused by the four balls need to be managed so not to cause the failure initiation, and the produced stress state at failure is somewhat complex making fractography somewhat challenging. Lastly, the ring-on-ring configuration is simple, but needed to be adapted (i.e., support ring size diameter approaching the 10 mm plate width) to cause tensile stress creation at the edges. Normally this is avoided for ring-on-ring testing because edge-induced fractures can undesirably affect strength results. Additionally, if there are differences in the two surfaces of the chips, then two test sets need to be generated.

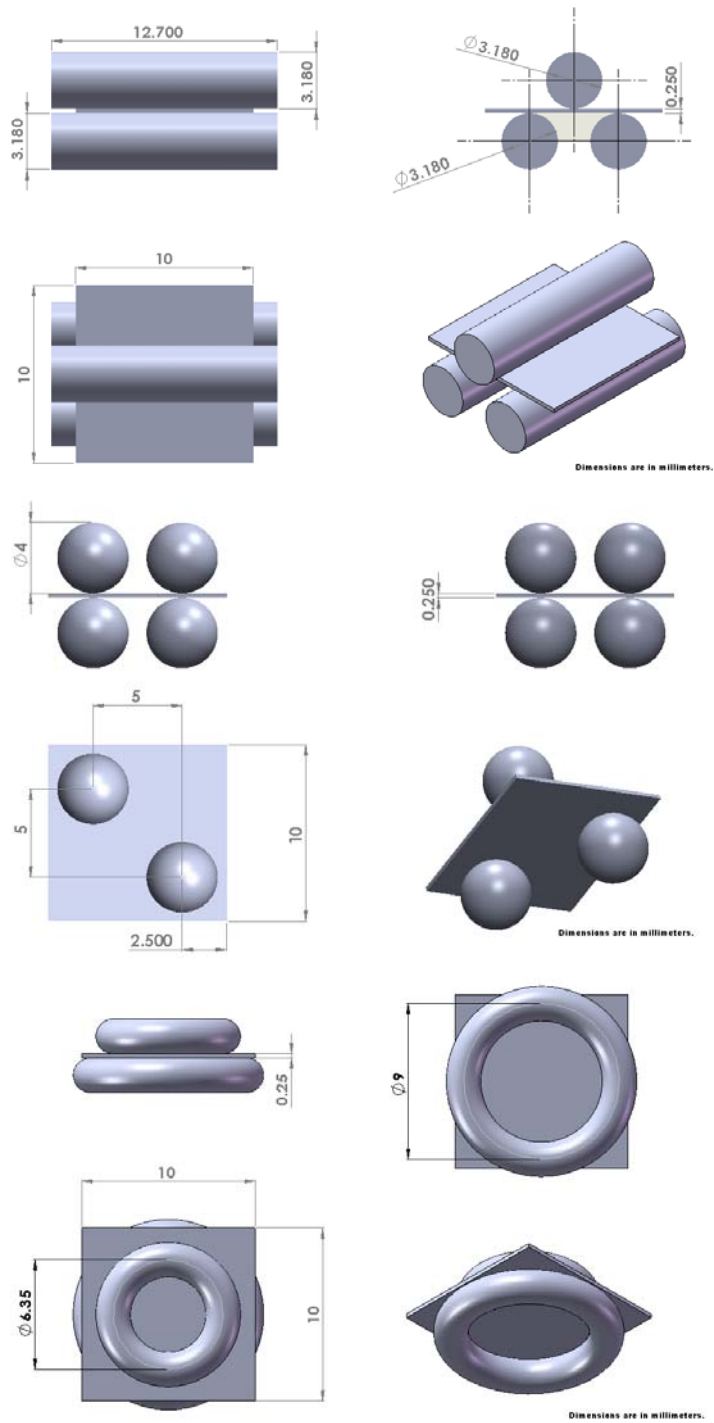
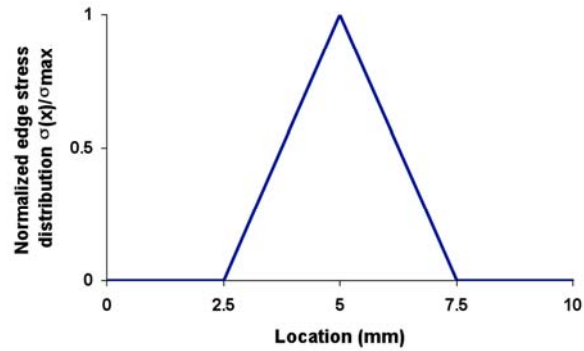


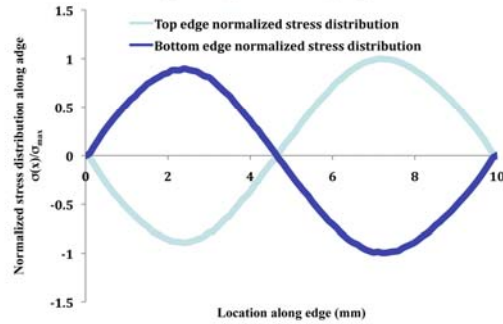
Figure 1. Three test configurations were sought to measure strength of the silicon and silicon carbide chips when the strength is limited by edge-located flaws. Three-point-bend (top), anticlastic bending (middle), and ring-on-ring (bottom) configurations shown.

$$L_{e,3\text{-point}} = \frac{2L}{m+1}$$



$$L_{e,AC} = 4 \left[ \int_0^{x1} \left( \frac{\sigma_{\text{bottom\_edge}}(x)}{\sigma_{\text{max}}^m} \right) dx + \int_{x1}^{10} \left( \frac{\sigma_{\text{top\_edge}}(x)}{\sigma_{\text{max}}^m} \right) dx \right]$$

$\sigma(x)$  expressions obtained by fitting 9<sup>th</sup> order polynomials to curves below



$$L_{e,ROR} = 4 \left[ \int_0^{10} \left( \frac{\sigma(x)}{\sigma_{\text{max}}} \right)^m dx \right]$$

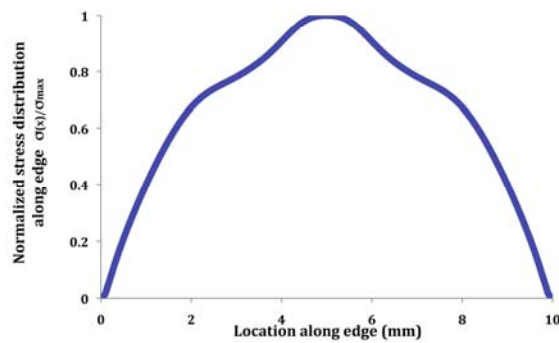


Figure 2. Resulting stress distributions along edges of the three-point-bend (top), anticlastic bending (middle), and ring-on-ring (bottom) configurations.

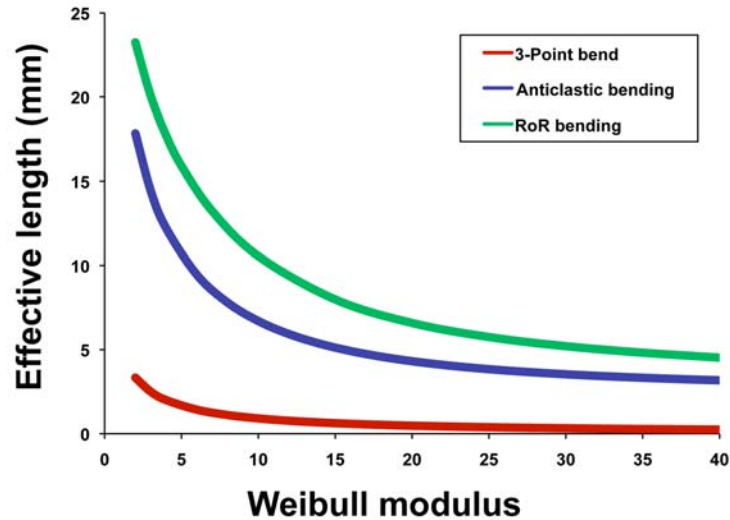


Figure 3. Effective length as a function of Weibull modulus for the three test configurations.

**Status of FY 2009 Milestones**

Compare cooling efficiencies in a hybrid inverter IGBT that contains contemporary and alternative ceramic DBC substrates. (09/09) *On schedule.*

**Communications/Visits/Travel**

Wereszczak attended the Vehicle Technologies Program Advanced Power Electronics and Electric Machines FY09 Kickoff Meeting, Knoxville, TN, November 18-19.

Wereszczak visited J. Gibbs at DOE HQ, Washington, DC on December 3 to discuss updates on this project.

Wereszczak visited USCAR, Southfield, MI, on December 4, and gave a presentation entitled "Enabling Higher-Temperature Operation and Improved Reliability in Automotive Power Electronic Devices" to the EE Tech Team.

**Problems Encountered**

None.

**Publications/Presentations/Awards**

None.

**References**

None.

## **Agreement 16305: Materials by Design – Solder Joints of High Performance Power Electronics**

**G. Muralidharan, Andrew Kercher, and Burak Ozpineci  
Oak Ridge National Laboratory**

### **Objective/Scope**

Advanced hybrid and electric propulsion systems are required to achieve the desired performance and life targets set for future automobiles. As specified in the OFCVT objectives, a target lifetime of 10-15 years has been projected for hybrid and electric propulsion systems meant for operation in harsh automotive environments. Power electronic components and systems are integral components of advanced automotive hybrid and electric propulsion systems. The trend in automotive power electronics is for using higher operating temperatures which has a detrimental effect on the stability of materials used in such systems. The objective of this task is to evaluate the effects of the higher temperatures on critical metallic materials that are used in power electronic devices and systems and to use the Materials-by-Design approach to identify appropriate combinations of materials that would decrease inopportune failures and maximum lifetime and reliability.

Based on the trend for using higher temperatures in power electronic components, there is a significant need to study failures of electronic packages induced by metallurgical changes of solder joints used as die attaches, and in wire bonds exposed to high temperatures ( up to 200°C in contrast to the current 125-150°C exposure) anticipated in such applications. These failures can be induced in solder joints and other components by combination of temperatures, stresses, and current. Coarsening of solder joint microstructure along with the formation of intermetallic compounds takes place during high temperature exposure. Wire bonds are also known to be a key location of failures for packages meant for high temperature use. An understanding of the failures in solder joints and wire bonds will empower us to develop a computation-oriented method for the design of materials for packaging applications.

The approach used in this work would be to study failures in simple package designs so that the emphasis is on materials rather than package design thus avoiding complexities of package design issues that may overshadow materials issues. Packages will be subject to extremes of operational stress levels/temperature levels to the study the origin of failures. Steady-state exposure at high temperatures and cyclic exposures (thermal fatigue) all affect microstructure of the materials, their properties, and hence the failure of joints. X-ray radiography along with acoustic and infrared imaging (as is necessary) will be used to characterize voids present in the solder joints. Knowledge from the failures would enable the selection/development of more appropriate materials that would ensure required lifetimes of 10 to 15 years expected of modules in EVs and Hybrid systems.

### **Technical Highlights**

In this quarter, in collaboration with Powerex Inc., progress has been made in preparing the first four solder joints for thermal cycling testing and high temperature exposure. Figure 1 shows an image of a 2.5 mm x 2.5 mm Silicon die mounted on a metallized

AlN DBC substrate with the metallization consisting of a medium phosphorus (6-12%) Nickel layer followed by a thin Au layer on the surface. 80Au/20Sn was the solder used for attaching the silicon die to the substrate. To understand the initial void content in the solder joint, high resolution x-ray radiography was carried out on the specimens. Figure 2 shows the image obtained from the same joint shown in figure 1. Light areas indicate the presence of voids. The joints will now be subject to thermal cycling to understand the evolution of the voids in the specific joints. Further effort will be made by PowerEx to reduce the void content.

#### **Status of FY 2008 Milestones**

Work is on schedule to meet the following milestone.

Complete thermal cycling testing on solder joints prepared with Au-Sn solder and two different substrate metallizations (9/09)

#### **Communications/Visits/Travel**

Frequent communications are being carried out with PowerEx to evaluate methodologies and to evaluate progress in understanding the behavior of solder joints.

#### **Problems Encountered**

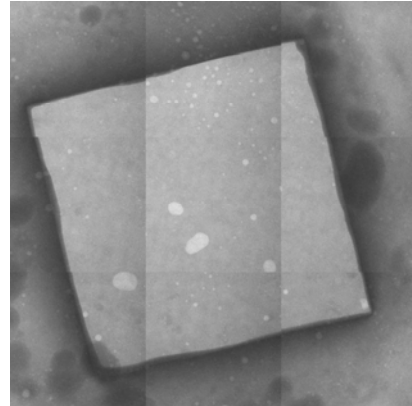
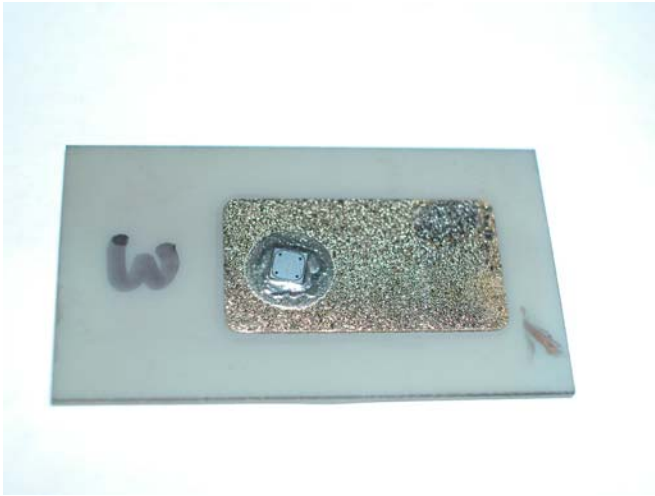
None

#### **Publications/Presentations/Awards**

None

#### **References**

None



(a) (b)  
Figure 1 (a). Image of the die attached assembly showing the die and the substrate. (b) High resolution x-ray image of a typical processed solder joint. The size of the chip is 2.5 mm x 2.5 mm.

**Agreement 16306: Materials Compatibility of Power Electronics**  
**B. L. Armstrong, D. F. Wilson, C. W. Ayers, and S. J. Pawel**  
**Oak Ridge National Laboratory**

**Objective/Scope**

The use of evaporative cooling for power electronics has grown significantly in recent years as power levels and related performance criteria have increased. As service temperature and pressure requirements are expanded, there is concern among the Original Equipment Manufacturers (OEMs) that the reliability of electrical devices will decrease due to degradation of the electronic materials that come in contact with the liquid refrigerants. Potential forms of degradation are expected to include corrosion of thin metallic conductors as well as physical/chemical deterioration of thin polymer materials and/or the interface properties at the junction between dissimilar materials in the assembled components. Initially, this new project will develop the laboratory methodology to evaluate the degradation of power electronics materials by evaporative liquids.

**Technical Highlights**

A laboratory test system that allows for high current flow and shaping of the wave form was designed and built in quarter three of FY08 and was operated for approximately 383.65 hours. This operating time equates to about 690,570 cycles. It was shut down during the first quarter for post-mortem evaluation of the circuit boards that are being tested. One board was removed, and the board was replaced and the test system is being prepared for resumption of operation. A thermocouple is being fashioned and will be inserted near the wires on one of the boards. The system will be restarted using the previous conditions [consisting of a square wave of one second on and one second off driving 10 amperes through 0.4 mm (400 microns) diameter aluminum wire] to allow for a determination of the temperature being experienced by the wires during the test cycle. Following this, the operating conditions of the test system will be changed to further stress the boards so that failure mechanisms can be expressed. This expression of failure is highly desired so that the limits of performance of the electronic board can be defined and the severity of testing necessary for rapid determination of performance can be ascertained.

**Status of FY 2009 Milestones**

Validate the proposed methodology for examining the interaction of the electrical components with evaporative coolant. **(09/09)** On track.

**Communications/Visits/Travel**

None to report.

**Problems Encountered**

None to report.

**Publications/Presentations/Awards**

None to report.

**References**

None to report.

## **Agreement 11752: Advanced Materials Development through Computational Design for HCCI Engine Applications**

**Govindarajan Muralidharan, Rick Battiste, and Bruce G. Bunting  
Oak Ridge National Laboratory**

### **Objectives/Scope**

To identify and catalog the materials operating conditions in the HCCI engines and utilize computational design concepts to develop advanced materials for such applications.

### **Highlights**

### **Technical Progress**

#### **Materials-by-Design of Advanced Materials:**

In this quarter, work was continued on Ni-based alloys for valve applications. As reported earlier, using thermodynamic modeling, microstructure evaluation, and mechanical property evaluation, high temperature fatigue was identified as a property of critical interest in Ni-based alloy valve materials for the next generation automotive engines. An important part of the on-going work is the development of a database of mechanical properties as a function of alloy composition and microstructure (which is a function of processing and heat-treatment). One of the issues relevant to this work has been the relationship between data collected using a rotating beam fatigue system and data obtained using fully reversed fatigue tests. To enable this comparison, and as requested by our industrial partner, fatigue data was obtained in currently used valve alloys at various stresses at a temperature of 760°C. Figure 1 shows a comparison of the fatigue life obtained at various stresses at two different temperatures. ORNL has recently acquired a rotating beam fatigue test system and data will be obtained on the same alloys under conditions identical to that used for fully reversed tests to enable comparison. Rotating beam fatigue data obtained at ORNL will also be compared with that available from our industrial partner.

#### **High Magnetic Field Treatment of Steel Components (with assistance from Dr. G. Ludtka and Dr. J. Wilgen)**

One of the techniques available for manipulation of material microstructure is that of high magnetic fields. High magnetic fields have been shown to influence phase equilibria in steels. At the request of another industrial partner, the effect of high magnetic fields on components fabricated from two different steels was evaluated. Of particular interest was the desire to transform the retained austenite present in these steels to martensite using large magnetic fields instead of the commonly used cryogenic treatment. One of the major factors that influenced the outcome of the experiments was that these components were supplied by our industrial partner and prior heat-treatments (austenitization and quenching) were conducted at least six months prior to the investigations conducted on the effect of magnetic fields on retained austenite contents.

Two components supplied by our industrial partner are shown in Figure 2. Figure 2 (a) shows the image of a fuel injector body comprising of 52100 steel while figure 2 (b) shows the image of a plunger made of M2 steel. Retained austenite contents in these components were evaluated by AMERICAN STRESS TECHNOLOGIES, INC, Cheswick, PA, using X-ray diffraction techniques. Following these measurements, the steel components were exposed to high magnetic fields. Figure 3 shows an image of the equipment specially fabricated to hold these specimens in a high (20 Tesla) magnetic field. Experiments were performed at the National High Magnetic Field Facility at Florida State University, Tallahassee, Florida. Effect of different field strengths and time varying magnetic fields on the retained austenite levels were the subject of the study. Retained austenite levels were measured in the same identified locations on each of the components after the conclusion of the high magnetic field exposure. Results show that the magnetic field may have some influence on the retained austenite levels in one of the steels even after significant time following the initial quenching treatment; this merits further experimental evaluation.

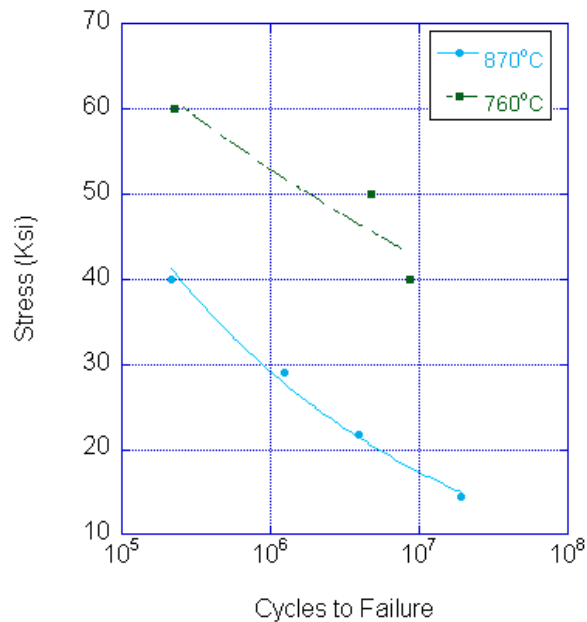


Figure 1. Fatigue life of the currently used valve alloy as a function of stress at 870°C and 760°C. Lines are drawn as a guide to the eye.



(a)



(b)

Figure 2. (a) Fuel injector body and (b) fuel injector plunger used to study the effect of high magnetic fields on the retained austenite levels present in the components.

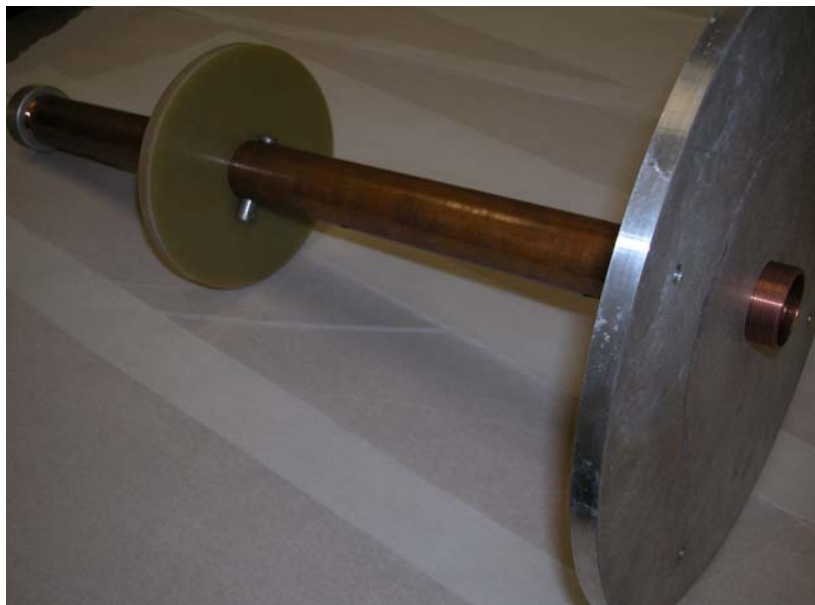


Figure 3. Fixture fabricated to hold components shown in Figure 2 in high magnetic fields. Specimens were placed inside the hollow copper tube shown in the figure. The aluminum plate was used to suspend the whole fixture from the top of the magnet while the G10 disk allowed the whole fixture to be retained in the center of the bore of the magnet resisting the large forces created by the magnetic field.

---

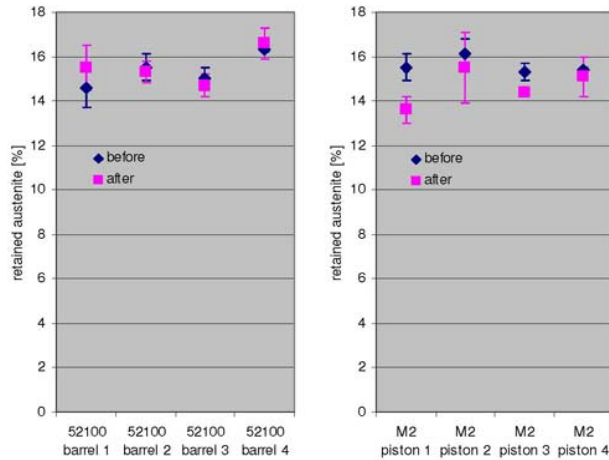


Figure 1: Comparison of retained austenite values for the barrels (left) and pistons (right) before and after magnetic processing. The 52100 barrels do not show a clear change due to the magnetic treatment. The M2 piston measurements suggest a slight reduction in austenite content. However, this effect is only on the order of 1% or less – similar to the level of expected variation. The error bars shown are the deviations from the calculation. They represent deviations among four values (“individual” retained austenite values), calculated from each ratio between the two ferrite/martensite and the two austenite peaks we measured.

Figure 4. Summary of results from a report provided by American Stress Technologies shows that the magnetic fields may reduced the retained austenite levels in M2 steels but needs further evaluation to confirm effects.

### Milestones

Evaluate fatigue properties of the most promising alternate alloys available and select best alloy for component fabrication/testing **(9/09)**

## **Agreement 16303: Materials for High Pressure Fuel Injection Systems**

**Peter J. Blau, Camden R. Hubbard, and Amit Shyam  
Oak Ridge National Laboratory**

**Michael J. Pollard, Ally Stahl, and Jeff A. Jensen  
Caterpillar Corporation**

### **Objective/Scope**

The objective of this Cooperative Research and Development Agreement (CRADA) between UT-Battelle, LLC and Caterpillar Corporation is to advance the state of the art in the characterization, selection, and use of metallic alloys for use in high-pressure diesel engine fuel injector nozzles.

During recent decades, fuel efficient, low-emissions diesel engine designs for heavy trucks have relied upon increasing fuel injection pressures to optimize combustion characteristics. Precise fuel metering is required. This key functional requirement has raised concerns over the ability of spray holes to be machined to sufficiently close tolerances to provide desired spray patterns and for the materials to withstand millions of high-pressure pulses without succumbing to fatigue damage. To achieve the purposes of this CRADA, a three-year effort is planned. The data and analyses obtained in the course of this work are expected to provide vital information for designers of high-performance fuel systems for advanced, energy-efficient diesel engines.

The effort began in the summer of 2008 with the development of a working plan involving three avenues of approach: (1) characterization of current fuel injector hole geometry and alloy metallurgy, (2) residual stress analysis of the nozzle tips in the location of the spray holes, and (3) the development and use of fatigue test methodology and analysis to address the special requirements of the next generation of high-pressure fuel injectors.

### **Technical Highlights**

*Nozzle characterization.* Several sets of fuel injectors, in various stages of production, were supplied to ORNL by Caterpillar Corporation. These were measured and photographed at varying magnifications and angles as an aid in both metallographic studies and residual stress studies using x-ray and neutron diffraction methods.

Optical microscopy and scanning electron microscopy was performed on the spray holes. Polished cross-sections were prepared to study the mechanical properties and microstructures of the alloy that is currently used. Due to the heat treatments and finishing methods that were employed in preparing the nozzles, the microindentation hardness near the free surfaces increased by about 20% relative to that at the center of the nozzle wall (see Figure 1).

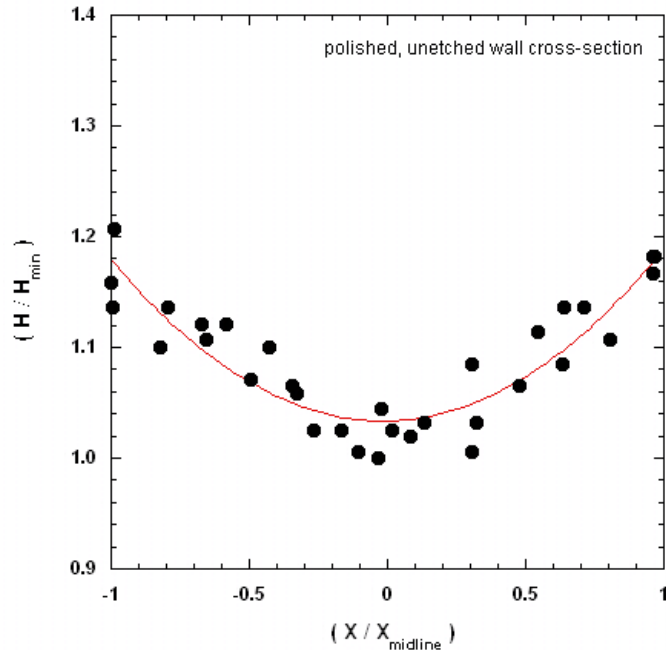


Figure 1. Indentation hardness profile through the wall of a fuel injector. Hardness data are normalized to the lowest value measured at the center of the wall and distance is relative to the center of the wall.

Preliminary etching studies, using several compositions of metallographic etchants designed for ferrous alloys, were conducted in order to evaluate the physical metallurgy of the nozzle materials and their phase composition. A thorough understanding of the processing effects on microstructure was needed to understand the material's propensity to resist fatigue crack initiation and propagation at high fuel injection pressures. The interpretation of etched microstructures obtained by optical and scanning electron microscopy is on-going and calls upon additional staff at ORNL with experience in steel metallurgy and heat treatments.

*Residual stress studies.* Residual stress can provide information on whether there are significant levels of residual stress at the surface and through the thickness. Initial trials were run by C. Hubbard who traveled to the National Synchrotron Light Source (NSLS), Brookhaven National Laboratory and also used the High Flux Isotope Reactor (HFIR) at ORNL. The purposes of the preliminary work were two-fold: (a) to determine the capabilities and limits to spatial resolution of synchrotron x-ray beam line X14A at NSLS to measure surface residual stresses in nozzle, particularly near the holes, and (b) to determine capabilities and limits to spatial and strain resolution of through-thickness stress mapping using the ORNL-HFIR neutron diffraction beam line.

At the NSLS, four nozzles, representing different stages of manufacturing, were examined. This high flux facility is optimized for polycrystalline diffraction (see Figure 2). Both hoop and radial stress measurements were made. The X14A beam line standard configuration limited the beam size to approximately 0.5 mm tall and 1 mm

wide. Using nominal mechanical properties of ferrous alloys, and the diffraction data, it did not appear that there were significant levels of residual stress in the parts.



Figure 2. Beamline at NSLS showing the four-circle goniometer with chi and omega tilt options.

At the HFIR, a second generation neutron stress mapping facility was used (see Figure 3). The beam slit was slightly smaller than that for the NSLS x-ray beam (0.5 x 0.5 mm), so the similar resolution and through thickness stress analysis are advantages. In order to assess the magnitude of the residual stresses, it was necessary to obtain strain-free specimens of the same material. Steep gradients near the nozzle surface made measurements difficult.



Figure 3. Neutron residual stress mapping instruments at ORNL's HFIR.

At this writing, the data from the initial neutron diffraction experiments at NFIR are being processed, and while initial results for both methods are not conclusive, there remains an excellent potential to obtain key stress data for nozzles using both x-ray and neutron diffraction methods. However, a number of technical challenges remain to be solved before achieving this ability to characterize specimens as small as the tips of injector nozzles.

Finally, the feasibility of using x-ray micro-tomography to image the nozzle tips is being considered in conjunction with a capability that has higher accelerating voltages than the NSLS. These developments will be reported later.

*Fatigue testing methodology.* Amit Shyam has been investigating several possible methods to characterize the fatigue resistance of nozzle tips containing spray holes. The challenge is to find a technique that simulates the stress state in the nozzle tip while enabling sufficient sensitivity to investigate the effect of the spray holes. Initial plans involve using a dual approach with standardized axial and flexural fatigue techniques to obtain baseline data, and subsequently introducing holes that are produced in a similar manner to those used in production fuel injectors. The effects of temperature and fuel environments will be explored in current and candidate alloys. After testing details are agreed upon, they will be discussed in subsequent reports.

### **Future Plans**

- 1) Continue microstructural analysis and hole characterization on commercial fuel injector nozzles.
- 2) Continue exploration of residual stress measurement methods that are suitable for the tips of fuel injectors.
- 3) Obtain specimen materials and machine initial fatigue test specimens in preparation for room-temperature baseline tests without holes.
- 4) Identify promising, fatigue resistant alloys that could replace the current injector nozzle materials.

### **Travel**

C. Hubbard traveled to Brookhaven National Laboratory from October 29-November 2, 2008, to determine the capabilities of beam line X14A to resolve residual stresses in injector nozzle barrels and tips.

### **Status of FY 2009 Milestone**

- 1) Design and develop a method to conduct fatigue tests on small holes. **(6/2009)** – in process

### **Publications and Presentations**

None this period.

## **Agreement 16304: Materials for Advanced Engine Valve Train**

**P. J. Maziasz and N. D. Evans  
Oak Ridge National Laboratory**

**N. Phillips  
Caterpillar, Inc.**

### **Objective/Scope**

This is an ORNL CRADA project with Caterpillar, NFE-07-00995 and DOE OVT Agreement 16304, that began last year, and lasts for about 2.5 years. This CRADA project is focused on addressing the wear and failure modes of current on-highway heavy-duty diesel exhaust valves and seats, and then evaluating changes in valve-seat design and advanced alloys which enable higher temperature capability, as well as better performance and durability. Requests for more detailed information on this project should be directed to Caterpillar, Inc.

### **Highlights**

#### **Caterpillar, Inc.**

This quarter, Caterpillar has set up several new “Buettner-Rig” seat/valve wear test facilities, and is test new, modified J3 seat insert to measure and verify improvements in initial wear resistance. Last quarter Caterpillar implemented evaluation of several new advanced valve alloys with one of its valve suppliers, and this quarter, the supplier is acquiring the appropriate materials for testing and evaluation at ORNL, as well as valve component trials and testing at Caterpillar.

### **ORNL**

ORNL continued in-depth microcharacterization studies of wear-tested valves and seats, and completed evaluation of a valve rig-tested for 360h at 740°C, to compare with previous data from similar valve testing at 850°C. These studies include comparison of high-wear and non-wear on the same rig-tested valves, as well as valve-alloys specimens aged at the same temperatures at ORNL, to clearly establish the degradation mechanisms at the surface and sub-surface valve regions.

### **Technical Progress, 1st Quarter, FY2009**

#### **Background**

This is a new ORNL CRADA project with Caterpillar, NFE-07-00995 and DOE OVT Agreement 16304, that began earlier this year, and will last for about 2.5 years. This CRADA project is focused on addressing the wear and failure modes of current on-highway heavy-duty diesel exhaust valves and seats, and then on evaluating changes in valve-seat design and/or advanced alloys that enable higher temperature capability, as well as better performance and durability. The need for such upgraded valve-seat alloys is driven by the demands to meet new emissions and fuel economy goals which continue to push diesel exhaust component temperature higher. Requests for more detailed information on this project should be directed to Caterpillar, Inc.

### **Approach**

Caterpillar will provide and analyze the baseline wear and mechanical behavior characteristics of engine-exposed valves and seats, and similar exposure of those components to laboratory simulation-rig testing at Caterpillar. ORNL will provide more in-depth characterization and microcharacterization of those valves and seats. Data will provide the understanding of the underlying degradation mechanism, and then also provide the basis for selecting and testing valve and seat alloys with upgraded performance. Caterpillar and ORNL are working with Caterpillar's various component or materials suppliers, so that potential solutions are commercially viable, and so that prototype components are readily available for Caterpillar's test rig or diesel engine evaluation.

### **Technical Progress – Caterpillar, Inc.**

Caterpillar and their major seat-insert supplier last quarter both performed the initial evaluations of modified processing to J3 seat inserts that showed initial resistance to several different modes of wear found previously. Last quarter and this quarter, Caterpillar complete improvement and expansion of their wear-testing capabilities, based on the "Buettner Rig" design, and have now begun testing and evaluation of seats with modified processing to mitigate lower temperature wear. Testing will continue into next quarter.

Last quarter, Caterpillar initiated a project with one of its valve suppliers to obtain several heats of advanced alloys for exhaust valves that should have improved performance and higher temperature capability relative to the current production alloy. This quarter, the valve supplier is obtaining those alloys, and will provide valve precursor material for ORNL to test and evaluate for mechanical properties and microstructural behavior, as well as prototype new exhaust valves for Caterpillar to test and evaluate in the wear-test rigs.

### **Technical Progress – ORNL**

ORNL continued in-depth microcharacterization studies of wear-tested valves and seats, and completed evaluation of a valve rig-tested for 360h at 740°C, to compare with previous data from similar valve testing at 850°C. These studies include comparison of high-wear and non-wear on the same rig-tested valves, as well as valve-alloys specimens aged at the same temperatures at ORNL, to clearly establish the degradation mechanisms at the surface and sub-surface valve regions.

### **Communications/Visits/Travel**

Detailed team communications between ORNL and Caterpillar occur regularly in multi-party conference calls. Caterpillar has extended team discussions to include their commercial seat-insert supplier as well as one of their exhaust valve suppliers.

### **Status of Milestones (ORNL for DOE)**

Perform the initial microanalysis of modified valves and/or seats after simulation-rig testing to evaluate wear-reduction (due Dec., 2008, delayed until June, 2009) – Status –

Delayed, but still in progress, due to delays and down-time of “Buettner-Rig” facilities at Caterpillar.

**Publications/Presentations/Awards**

None

## **Agreement 13329: Design Optimization of Piezoceramic Multilayer Actuators for Heavy Duty Diesel Engine Fuel Injectors**

**Hua-Tay Lin, H. Wang and A. A. Wereszczak  
Oak Ridge National Laboratory**

**D. W. Memering and J. Carmona-Valdes  
Cummins Inc.**

### **Objective/Scope**

Enable confident utilization of piezo stack actuator in fuel injectors for heavy vehicle diesel engines. The use of such actuators in diesel fuel injectors has the potential to reduce injector response time, provide greater precision and control of the fuel injection event, and lessen energy consumption. Though piezoelectric response is the obvious primary function of lead zirconate titanate (PZT) ceramic stacks for fuel injectors, their mechanical reliability can be a performance and life limiter because PZT is brittle, lacks high strength, and is susceptible to fatigue. However, that brittleness, relatively low strength, and fatigue susceptibility can be overcome with the use of appropriate probabilistic design methods.

### **Technical Highlights**

#### **1. Piezoceramic Characterization**

A commercially available material was examined in this study, PSI-5A4E (Piezo Systems, Inc., Cambridge, MA). This material designated as PZT-5A in industry has high piezoelectric coefficients ( $d_{33} = 390$  pC/N,  $d_{31} = -190$  pC/N) and a high Curie temperature (350°C); therefore, it is an excellent candidate for engine fuel injection application. Our previous investigation has shown that both the sign and the magnitude of an electric field had a significant effect on the mechanical strength of the poled PZT [1], whilst that effect was studied only within the coercive field level of the material. It appears to be imperative to include a large range of electric field into this testing matrix. This is significant because piezoelectric industries currently use a field level higher than the coercive strength of PZT material in their product to achieve a desired stroke. But no related data are available that can provide insight into the effect of such high electric field on the mechanical performance of piezoceramic.

A total of 60 PZT specimens prepared out of four sheets were used in testing. These specimens were sized with 10 mm x 10 mm x 0.267 mm, and their surface and poling conditions were same as before [1]. However, the specimens were randomly selected during testing among those of each sheet to reduce the sheet-to-sheet variation. The ball-on-ring testing configuration and procedure have been detailed in ref. 1. Same designation is used in this report to signify the test condition, xxx-xx; the first part indicates the electrode orientation with respect to the tensile surface of flexure specimen (PoT or NoT), and the second part gives the electric load (OC, 1.2 and 2.4 kV/mm).

The strength results for PoT-OC along with those for various PoT and NoT electric conditions are presented in Fig. 1 (a) and (b), respectively. It can be seen that a positive field of 1.2 kV/mm enhanced the strength and a negative one reduced it, and that was similar to the results in the reference [1]. It has been observed that the Weibull modulus,  $m$ , appeared to be relatively larger ( $m = 23$  to  $28$ ) under both the OC and the  $-1.2$  kV/mm than that of  $1.2$  kV/mm ( $m = 12$ ). Similar value of Weibull modulus was also observed in our earlier tests on a different batch of PZT sheets. It remains unknown if this means a different population of flaws was involved, but it is worthwhile to mention that a flaw can behave differently under the influence of electric field [1].

Increasing the electric level to  $2.4$  kV/mm in positive direction resulted in the further enhancement in the mechanical strength of poled PZT. The characteristic strength appeared to be  $171$  MPa that was relatively larger than that obtained under  $1.2$  kV/mm, although it is not statistically significant (overlaid estimate intervals existed with 95% of confidence level). Apparently, an increased electric field forced more domains to be aligned along the considered crack plane. While the toughening depends on the domain switching around the crack tip, the increased amount of switchable domains would lead to a more energy dissipation and more increase in fracture toughness. This increased toughness was reflected in the observed trend in mechanical strength with the applied electric field.

On the other hand, increasing in the negative direction of electric field to  $2.4$  kV/mm resulted also in an increase but not a continual decrease in the mechanical strength of poled PZT. The characteristic strength appeared to be  $169$  MPa that is comparable to that obtained under  $+2.4$  kV/mm. Apparently, the increased electric field in the negative direction forced the domains to be re-aligned along the considered crack plane as well, and thus again the increased amount of switchable domains led to the toughening and the increased mechanical strength.

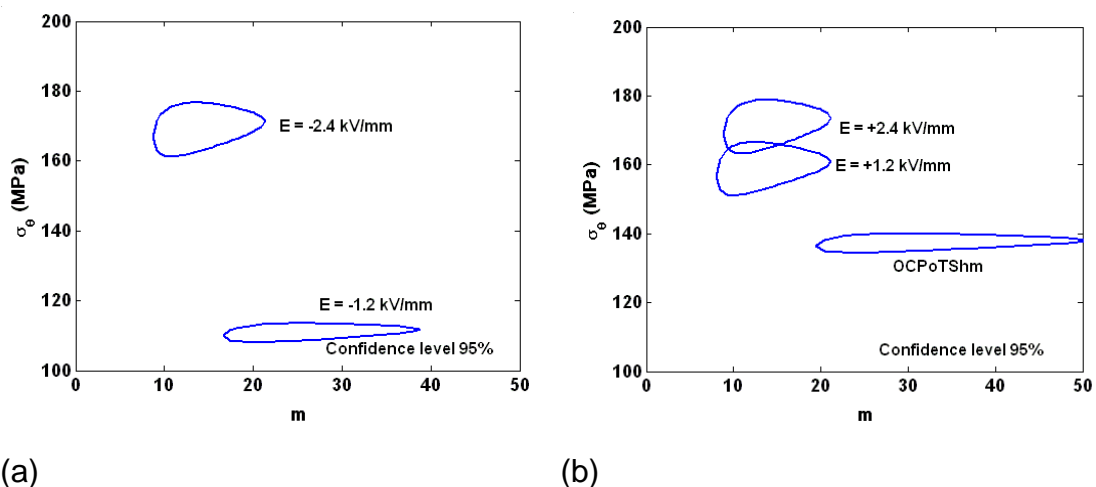


Fig. 1. Confidence ratio rings (95% confidence level) for (a) NoT-1.2 and NoT-2.4; (b) PoT-OC, PoT-1.2 and PoT-2.4. The nominal specimen size is  $10.0$  mm  $\times$   $10.0$  mm  $\times$   $0.267$  mm, the loading ball diameter is  $2.00$  mm and the inner diameter of supporting ring is  $7.444$  mm.

## 2. Piezoceramic Multilayer Actuator Characterization

Tested stacks were purchased from Noliac (Denmark). They had an overall size of 5mm x 5mm x 18mm and were composed of 8 active plates (modules) and 2 dead endplates. The experimental set-up of ORNL piezostack fatigue test facility was provided in details in the ref. 1.

Our previous study showed that the strain and piezoelectric hysteresis of tested PZT stacks were reduced markedly after  $10^8$  cycles. Moreover, No. 05 had a much more significant and earlier drop than No. 02 (Fig. 2). As a result of that, more testing was suggested and conducted under same cycling condition in this period. The result for No. 07 was included and given in Fig. 2 along with other two.

Stack No. 07 appeared to have an immediate reduction level between those of No. 02 and 05. A fast drop was exhibited around  $10^7$  of cycles in both the strain and piezo hysteresis, corresponding to a stage when extensive surface discharges emerged on both positive and negative electrode surfaces of the stack. About 40% decreases in these quantities were observed. The amount of variation was also quite similar for No. 07 in both the electric measuring mode (bipolar or unipolar).

Overall, the amount of reduction (24 to 45%) in mechanical strain induced by a semi-bipolar fatigue was considerably larger than that caused by a unipolar fatigue (~6%) [2]. That is quite significant, even though the mechanical preloads and electric field levels as well as frequencies were different in these fatigue tests. Detailed analysis via electron microscopy will be carried out to understand the degradation mechanism.

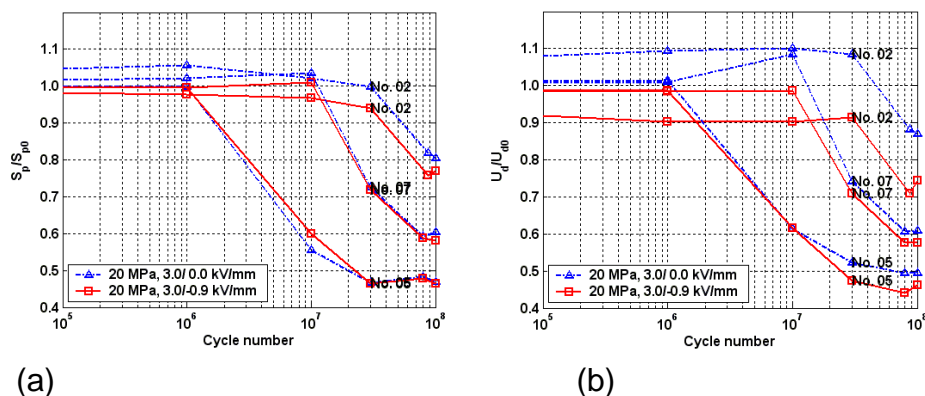


Fig. 2 Variations of normalized peak field-induced strain (a) and normalized piezoelectric hysteresis (b) for stack No. 02, 05 and 07, as a function of cycle number ( $10^5$ -  $10^8$ ). Mechanical and electric loading conditions in measurement are given in figures.

## Reference

1. H. Wang and A. A. Wereszczak, "Effects of Electric Field and Biaxial Flexure on the Failure of Poled Lead Zirconate Titanate," *IEEE Trans. Ultrasonic, Ferroelectrics, and Frequency Control*, 55 (12), 2008, 2559-2570.

2. H. Wang, A. A. Wereszczak, and H.-T. Lin, "Fatigue Response of a PZT Multilayer Actuator under High-field Electric Cycling with Mechanical Preload," *J. Appl. Phys.*, 105 (1), 2009, 014112.

### **Status of FY 2009 Milestones**

Measure and compare piezoelectric and mechanical reliabilities of tape-cast and pressed PZT piezoceramics. (09/09) on schedule.

### **Communications/Visits/Travel**

The CRADA kick-off meeting on "Mechanical Reliability of PZT Actuator" was held at Cummins on December 8, 2008.

### **Publications/Presentations/Awards**

1. Wang, H., Lin, H.-T., Wereszczak, A. A., and Cooper, T. A., Mechanical strain and piezoelectric properties of PZT stacks related to semi-bipolar electric cycling fatigue, submitted to *33<sup>rd</sup> Int. Conf. on Adv. Ceramics and Composites*, Jan. 18-23, 2009, Daytona Beach, FL.
2. Wang, H., Wereszczak, A. A., and Lin, H.-T., Fatigue response of a PZT multilayer actuator under high-field electric cycling with mechanical preload, *J. Appl. Phys.*, 105 (1), 2009, 014112.
3. Wang, H. and Wereszczak, A. A., Effects of electric field and biaxial flexure on the failure of poled lead zirconate titanate, *IEEE Trans. Ultrasonic, Ferroelectrics, and Frequency Control*, 55 (12), 2008, 2559-2570.

## **Agreement 13332: Friction and Wear Reduction in Diesel Engine Valve Trains**

**Peter Blau**  
**Oak Ridge National Laboratory**

### **Objective/Scope**

The objective of this effort is to enable the selection and use of improved materials, surface treatments, and lubricating strategies for valve train components in energy-efficient diesel engines. Depending on engine design and operating conditions, between 5 and 20% of the friction losses in an internal combustion engine are attributable to the rubbing between valve train components. Moreover, wear-induced leaks around valve seats can reduce cylinder pressure and engine efficiency while leading to increased emissions. This effort focuses on understanding the complex wear-oxidation processes that occur in the interface between diesel engine exhaust valves and seats. The knowledge gained is expected to help engine designers to select materials and surface treatments for increased reliability and reduced engine emissions.

FY 2007 witnessed the completion of a high-temperature repetitive impact (HTRI) testing system to test the surface durability of candidate exhaust valve materials at diesel engine temperatures. In FY 2008, the conjoint role of wear plus oxidation was investigated in more detail, establishing that oxidation products that form on mechanically-damaged surfaces differ from those on statically oxidized surfaces. Selected Fe-, Ni-, and Co-base alloys were used as model materials and resulted in two journal publications and a conference presentation. A high-temperature, repeated impact (HTRI) apparatus was designed in FY 2007 and completed in FY 2008. The development of that apparatus presented significant engineering challenges, and work continued on modifying the contact geometry to enable more consistent and quantitative measurements of corrosion-assisted wear effects at the high temperatures typical of exhaust valve operation. Results are shared on a continuing basis with U.S. diesel engine manufacturer who has also supplied production-grade exhaust valves for our studies. Finally, work continues on the validation of a new ASTM test method for piston ring and liner friction by means of an inter-laboratory testing project that involves participants in the U.S. and U.K.

### **Technical Highlights**

*Development of a high-stress, self-aligning contact geometry for high temperature repetitive impact testing of valve materials.* The ORNL high temperature, repetitive impact system (HTRI) was described in previous reports (see for example, the FY 2008 DOE/OVT Propulsion Materials Annual Report). The HTRI consists of a vertical oscillating drive that causes two pairs of specimens to repeatedly separate and come back together, imparting a combination of slip and impact due to its inclined contact geometry. Two standard configurations were developed. One uses actual exhaust valves impacting flat blocks, and the other uses simpler test coupons (inclined cylinders on inclined flat surfaces) that can be made from candidate alloys or surface treatments without the need to use full-sized valves. Both configurations, particularly the latter, presented difficulties for achieving consistent contact alignment. That made quantification of the contact damage problematic. Considerable effort was subsequently devoted to achieving more quantitative results. Toward the end of FY

2008, a new design that offers both higher contact stress (for accelerated testing) and more consistent self-aligning features was developed. Figure 1 (a) shows the former contact geometry, and Figure 1 (b) shows the new, higher-stress, self-aligning geometry. The new contact geometry employs subtle changes and allow for some play for block rotation under load. In this way, the new contact geometry becomes, in effect, a crossed-cylinders configuration, with one body having a contact radius ( $r_1$ ) of inclined cylindrical pin and the other body having a contact radius ( $r_2$ ) of the rounded corner of the test block.

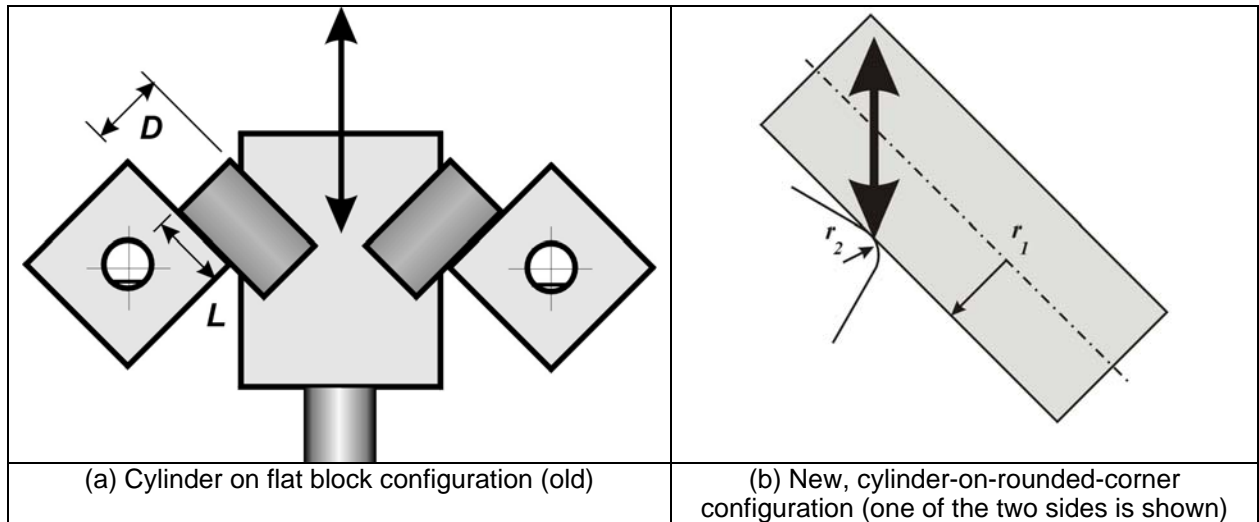


Figure 1. Comparison of testing geometries to improve alignment and increase the contact stress.

The 31 N down-force ( $P$ ) exerted on the contacts is due to the mass of the apparatus that hangs on the block specimens when the oscillating drive loses contact with bottom of the drive shaft. The normal force on the crossed-cylinders contact, due to the 45 degree incline is thus,  $P \sin 45^\circ$ , or 21.92 N. Assuming 9.525 mm diameter cylinders ( $r_1 = 4.763$  mm) and a rounded radius of the block ( $r_2 = 1.3$  mm), as measured by image analysis on block specimens, the maximum elastic compressive contact stress can be calculated using the equations of H. Hertz [1] for the case of a self-mated Ni-based valve alloy (elastic modulus = 207 GPa, Poisson's ratio = 0.28):

$$[\sigma_{\max}]_{\text{cyl/flat}} = 143 \text{ MPa}$$

$$[\sigma_{\max}]_{\text{crossed-cyl}} = 2080 \text{ MPa}$$

Thus, compared with the previous configuration, the new geometry increases the elastic stress by a factor of 14.5 and this, in turn, should lead to accelerated wear.

Figure 2 (a) shows the tear-drop-shaped wear scar on the rounded edge of a block specimen of a Ni-based alloy (Pyromet 80A™) tested using the geometry of Figure 1(b) for 20,000 contact cycles at room temperature against cylindrical pins of a Co-based alloy (Stellite 6B™). The higher-magnification light optical image in Figure 2(b) shows tiny fragments of metal and oxide produced under the subject test conditions. At elevated temperatures, the wear particles are expected to contain a mixture of

fragmented, high-temperature oxidation products. That research will continue during coming months with HTRI experiments at 750°C or higher.

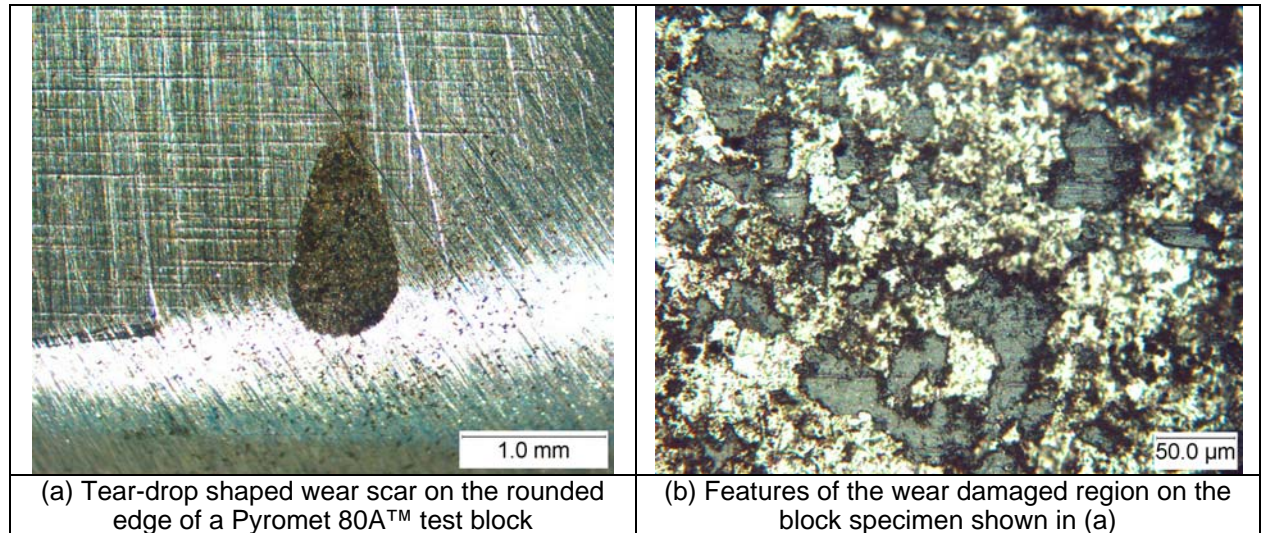


Figure 2. Wear damage due to 20,000 impacts on a Ni-based alloy against a Co-based pin material at room temperature.

### **Reference**

[1] W. C. Young (1989) *Roarks' Formulas for Stress and Strain*, 6<sup>th</sup> ed., McGraw-Hill Book Company, New York.

### **Future Plans**

- 1) Continue high-temperature, repetitive impact tests on the candidate alloys using the new, higher contact stress configuration and study the microstructures produced by combined impact, slip, and oxidation.
- 2) The principal investigator has been invited to present a keynote paper at a European conference focused on wear plus corrosion ('Tribo Corrosion 2009,' Wiener Neustadt, Austria).
- 3) Prepare and submit a paper describing the design of the high-temperature repetitive-impact system (see Milestone 1, below).

### **Travel**

None this period.

### **Status of FY 2009 Milestones**

- 1) Prepare and submit a journal article that describes the new high-temperature test method for diesel exhaust valve materials. **(03/09)**
- 2) Prepare and a final report or journal article that summarizes the role of wear with oxidation in controlling the durability of diesel engine exhaust valve materials. **(09/09)**

### **Publications and Presentations**

- 1) P. J. Blau and T. M. Brummett, "High-Temperature Oxide Regrowth on Mechanically-Damaged Surfaces", *Tribology Letters*, Vol. 32 (3), pp. 153-157
  
- 2) P. J. Blau, T. M. Brummett, and B. A. Pint, "Effects of prior surface damage on high-temperature oxidation of Fe-, Ni-, and Co-based alloys," accepted for the 2009 International Conference on Wear of Materials, Las Vegas, Nevada, April 19-22; also for publication in the journal *Wear*.

## **Agreement 17894: NDE Development for ACERT Engine Components**

**J. G. Sun and J. A. Jensen\***  
**Argonne National Laboratory**

**\*Caterpillar, Inc.**  
**Technical Center**

### **Objective/Scope**

Applications of advanced materials in diesel engines may enhance combustion and reduce parasitic and thermal losses, thereby improving engine efficiency. Engine components developed from advanced materials, however, require rigorous assessment to assure their reliability and durability in more stringent operating conditions. The objective of this work is to develop and assess various nondestructive evaluation (NDE) methods for characterization of advanced engine components in a Caterpillar heavy-duty ACERT experimental engine at ORNL. NDE technologies established at ANL, including optical scanning, infrared thermal imaging, ultrasonics, and X-ray CT, will be further developed for detection of volumetric, planar, and other types of flaws that may limit the performance of these components. NDE development will be focused on achieving higher spatial resolution and detection sensitivity. Current efforts are directed in applications of optical methods for valve train components, X-ray and ultrasonic for joinings, and thermal imaging for thermal barrier coatings (TBC).

### **Technical Highlights**

Work during this period (October-December 2008) focused on modeling thickness effect in radiography and on evaluating thermal tomography method for TBC characterization.

#### **1. NDE Inspection of Joints**

Radiography is a fast NDE method to inspect joint. For specimens with variable thickness, such as cylinder and rod, the x-ray transmission data display a large dynamic range due to the thickness variation, which may hinder the detection of detailed abnormality. Work is being conducted to correct the thickness effect in radiographs for cylindrical specimens. Results will be presented in the next report.

#### **2. Thermal Imaging for Thermal Barrier Coatings**

Thick thermal barrier coatings (TBC) have been developed by Caterpillar for insulation of materials for diesel engines capable of operating in advanced combustion cycles to reduce emission and improve efficiency. These TBCs range from one to several millimeters thick, and can be made of various materials including ceramics, amorphous steels or quasicrystals. Although NDE development for TBCs has been pursued for a few decades, driven by the turbine-engine industry, few NDE technologies are capable to even qualitatively characterize thick TBCs with wide thickness and material range. Among these, thermal imaging has been widely used for TBC inspection, although most of the applications are of qualitative nature and providing limited structural information. ANL has been active in developing new data-processing methods based on pulsed thermal imaging technology. Two methods are being developed: a thermal tomography method and a multilayer modeling method. The thermal tomography method can construct 3D images of material's thermal effusivity in an entire specimen volume, and

the multilayer modeling method may quantitatively determine thermal properties (conductivity and diffusivity) of the TBC layer; both can be used for NDE characterization of multilayer TBC materials. The thermal tomography method was tested in this period to characterize earlier TBC materials (ceramic) developed for diesel engines. Figure 1 shows a photograph of two TBC samples. The coating thickness is 1 mm for the left sample and 2mm for the right sample. The thicker TBC was also coated with a thin layer of black paint, which is a common practice for thermal imaging to increase detection sensitivity. Figure 2 shows typical plane-slice images of the thin TBC. It is apparent that some flaws exist at below  $\sim 0.5\text{mm}$  from the surface, and they appear to extend up to the interface (at 1mm deep) between the TBC and the substrate. The coating of the thicker TBC sample is relatively uniform (see Fig. 3), although a material pattern (of varying emissivity) emerges at below  $\sim 1.4\text{mm}$  from the surface. These results will be further investigated in next period.



Fig. 1. Photograph of 1-mm-thick (left) and 2-mm-thick (right) TBC specimen.

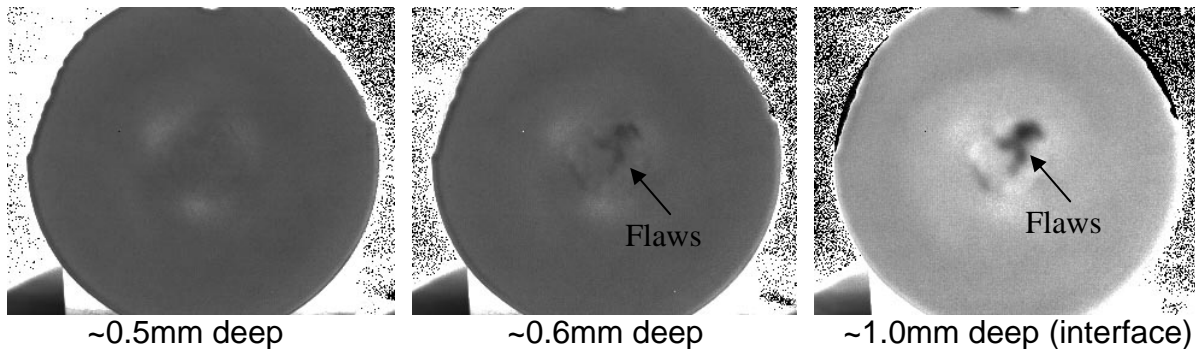


Fig. 2. Typical thermal tomography plane-slice images for a 1-mm-thick TBC sample.

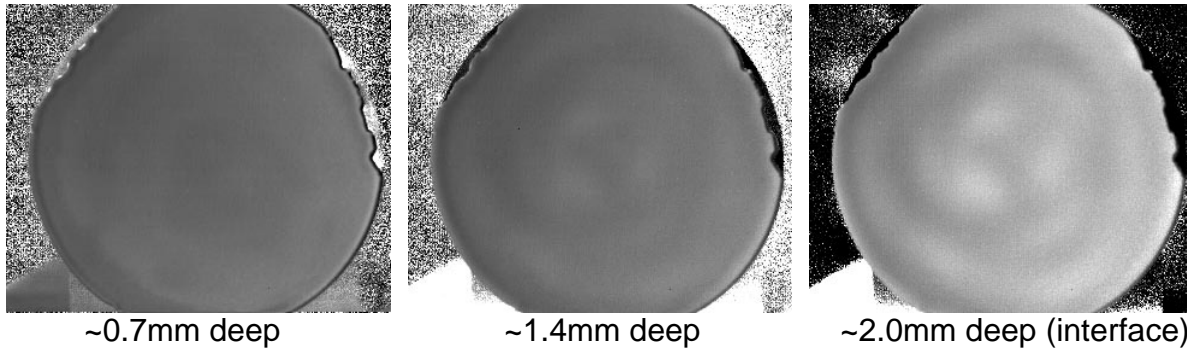


Fig. 3. Typical thermal tomography plane-slice images for a 2-mm-thick TBC sample.

### **Status of Milestones**

Current ANL milestones are on schedule.

### **Communications/Visits/Travel**

J. G. Sun plans to present two papers entitled “Nondestructive Inspection of Ceramic Bearing Balls Using Phased Array Ultrasonics” and “Measurement of Thermal Barrier Coating Conductivity by Thermal Imaging Method” at the 33<sup>rd</sup> International Conference on Advanced Ceramics and Composites to be held in Jan. 18-23, 2009 in Daytona Beach, FL.

J.G. Sun plans to visit Caterpillar in February 2009.

### **Problems Encountered**

None this period.

### **Publications**

A paper was submitted to International Journal of Applied Ceramic Technology. Its title is “Cross-polarization confocal imaging of subsurface flaws in silicon nitride,” co-authored by Zunping Liu, Jiayang Sun, and Z.J. Pei.

## **Agreement 15050: Materials-enabled High Performance Diesel Engines**

**M. D. Kass, R. Wagner, T. J. Theiss, and H. T. Lin**  
**Oak Ridge National Laboratory**

### **Objective/Scope**

This project is focused on improving the performance, emissions and efficiency of heavy-duty diesel engines through the application of materials enabled technologies. The range of material systems is comprehensive and includes 1) improved structural materials to accommodate higher cylinder pressures and temperatures, 2) improved durability and corrosion resistance, 3) low inertial components to improve transient response, 4) improved emissions aftertreatment performance, and 5) waste heat recovery systems.

### **Highlights**

The CRADA paperwork was finalized during this quarterly period. ORNL received the ECU communications adapter wiring harness. The C-15 ACERT engine is mounted on the dynamometer along with the accompanying infrastructure.

### **Technical Progress, 1st Quarter, FY2009**

#### **Background**

ORNL and Caterpillar are engaged in discussions to establish a CRADA in 2008 focusing on materials-enabled advancements to heavy duty diesel engines. Caterpillar has provided ORNL with a 2005 C-15 ACERT engine and two 600 hp DC motoring dynamometers to support this activity. Materials scientists at Caterpillar are working with their engine/combustion research staff to develop a pathway to combine materials expertise with engine research and development needs. A research team at ORNL comprising engine/combustion staff with materials scientists has held several discussions with Caterpillar staff to address issues and potential concerns. To help move this effort forward the Fuels, Engines, and Emissions group received \$900K of internal support to setup an engine test cell, dedicated to this effort, in a vacant room located at the NTRC building. Building modifications and equipment procurement has been initiated. The test cell is scheduled to be available for use in June 2008.

#### **Approach**

This unique activity will incorporate the materials research and engine/combustion expertise at Oak Ridge National Laboratory to investigate potential materials enabling technologies for heavy-duty diesel engines. Caterpillar has provided a C-15 ACERT engine for this effort and has also contributed two dynamometers. Caterpillar will provide technical support and oversight. Caterpillar engineers will also define the operating parameters to be studied. The specifics and details of the CRADA are currently being negotiated. Caterpillar and ORNL will work with Caterpillar's various component or materials suppliers so that potential solutions are commercially viable.

### **Communications/Visits/Travel**

ORNL and Caterpillar held a meeting at the 2008 Diesel Engine and Emissions Reduction conference. ORNL and Caterpillar have also initiated biweekly status teleconferences to facilitate communication between the two parties.

### **Status of Milestones (ORNL for DOE)**

CRADA paperwork is complete.

### **Publications/Presentations/Awards**

Mike Kass gave a presentation entitled "Materials-enabled High Efficiency Diesel Engines" at the DOE Annual Merit Review.

## **Agreement 9130: Development of Materials Analysis Tools for Studying SCR Catalysts**

**Thomas Watkins, Larry Allard, Michael Lance, Harry Meyer and Larry Walker  
Oak Ridge National Laboratory**

**Krishna Kamasamudram, Cheryl Klepser and Alex Yezerets  
Cummins Inc.**

### **Objective**

The objective of this effort is to produce a quantitative understanding of the interdependence between structure and performance to develop options for an exhaust after treatment system with improved final product performance in order to meet the US Environmental Protection Agency emissions requirements for 2010 and beyond.

### **Technical Progress**

A manifold was delivered to ORNL from Cummins in the Fall of 2008 (see Figure 1). The manifold consists of 5 mass flow controllers, a mass flow and pressure programmer and a piping circuit flowing through a water bubbler. The manifold was mounted onto a cart as shown in Figure 2, and now the mass flow controllers are being calibrated with a wet test meter. Four "half cylinders" of N<sub>2</sub>, O<sub>2</sub>, NO and NH<sub>3</sub> gas and corresponding regulators have been ordered and received. Once calibration is complete, these cylinders will be mounted on the cart behind the manifold panel. Next, the bubbler will be mounted onto the cart, and further testing will continue. This portable system will be moved as needed to various characterization instruments (e.g., x-ray diffractometers, piezo-spectrometers, microscopes or furnace) and plumbed in to provide simulated exhaust for in-situ measurements.

### **Microscopy**

High-resolution electron microscopy studies have been conducted on the suite of hydrothermally aged Fe-zeolite samples, utilizing HTML's aberration-corrected JEOL 2200FS STEM/TEM instrument (the "ACEM"). A major goal of our study has been to try to identify by imaging and possibly elemental microanalysis the location of Fe species within the cage structure of the zeolite material, which has been shown to be consistent with the basic structure of H-beta zeolite by XRD techniques. The ACEM, however, has not, until very recently, been equipped with an energy-dispersive x-ray analysis system, so intermediate results were obtained at first using the new cold-field emission 300kV Hitachi HF-3000 TEM/STEM instrument, which is an advanced capability analytical electron microscope equipped with a Noran energy-dispersive spectrometer. The HF-3000 can provide annular dark-field images similar to those obtained on the ACEM, but with a resolution of about 0.5 nm at best, using beam conditions suitable to also give reasonable x-ray imaging results.

Figure 3a shows an annular dark-field (ADF) image, recorded at 300kx, of the as-received Fe-zeolite material “before” simultaneous acquisition of a series of x-ray maps for the elements Al, Fe, and Si. Figure 3b is the same sample area “after” the analysis. The x-ray images were obtained with a scanning time of about 40 minutes, so the changes in the morphology of the zeolite in the “after” images are indicative of the effects of the electron beam on the structure. The characteristic structural feature seen is a distribution of bright patches in the ADF images that we have supposed are consistent with concentrations of Fe species, since annular dark-field contrast is essentially directly proportional to  $Z^2$ , where Z is the atomic number. Figure 4 shows the results of the x-ray mapping of this area. The Al and Si maps are essentially uniform in counts, as expected, whereas the Fe map shows an overall uniform distribution with several indications of concentrations (arrowed) consistent with corresponding bright patches in the ADF image. It is expected that higher magnification maps, as are soon to be possible with the new detector on the ACEM, will clarify further the Fe distributions.

A new x-ray detector was recently installed on the ACEM (See Figure 5). The detector was provided by Bruker AXS Inc. (Madison, WI), and is a new design of Silicon Drift Detector (SDD), which is typically used in high-count rate environments such as found on scanning electron microscopes and electron microprobes. The new SDD is designed to give good results on a TEM instrument, which, because of the typical thin sample (or nanoparticle) morphology will inherently give low count rates. Our Bruker SDD is the first of its kind to be commercially installed on a TEM in the US (only 3 currently in the world). We are testing this detector and will report on the efficacy of its use for analysis of catalytic materials in general, and our zeolites in particular, in a future quarterly report.

### **Meetings**

ORNL personnel traveled to the Cummins Technical Center and met with Cummins personnel on Thursday November 13, 2008 and again on Thursday December 4, 2008 to discuss the technical progress and future plans of this CRADA.

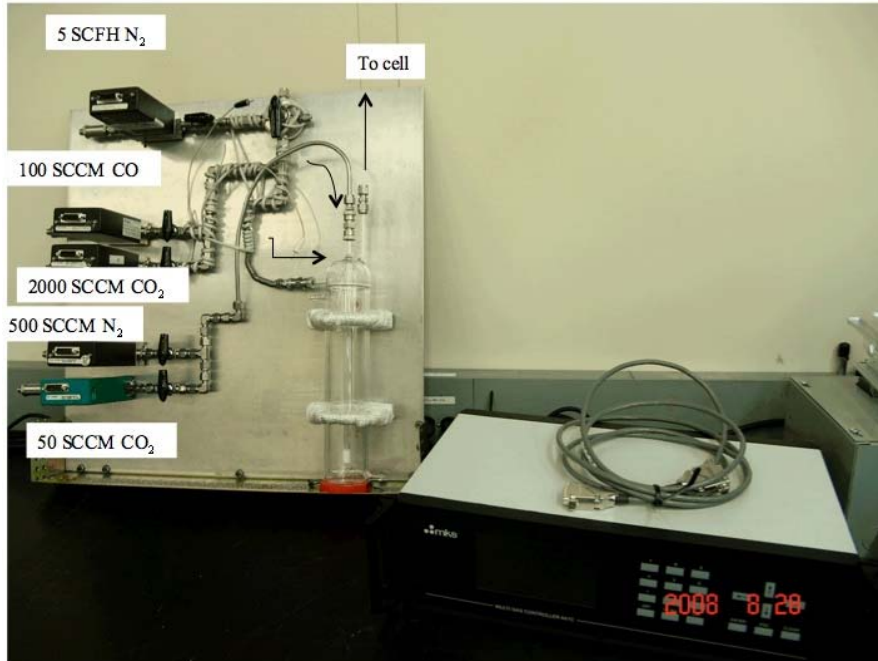


Figure 1- Manifold system with five mass flow controllers, mass flow and pressure controller and bubbler. Gases displayed are standard gases for each MFC and are not necessarily the gases to be used experimentally.

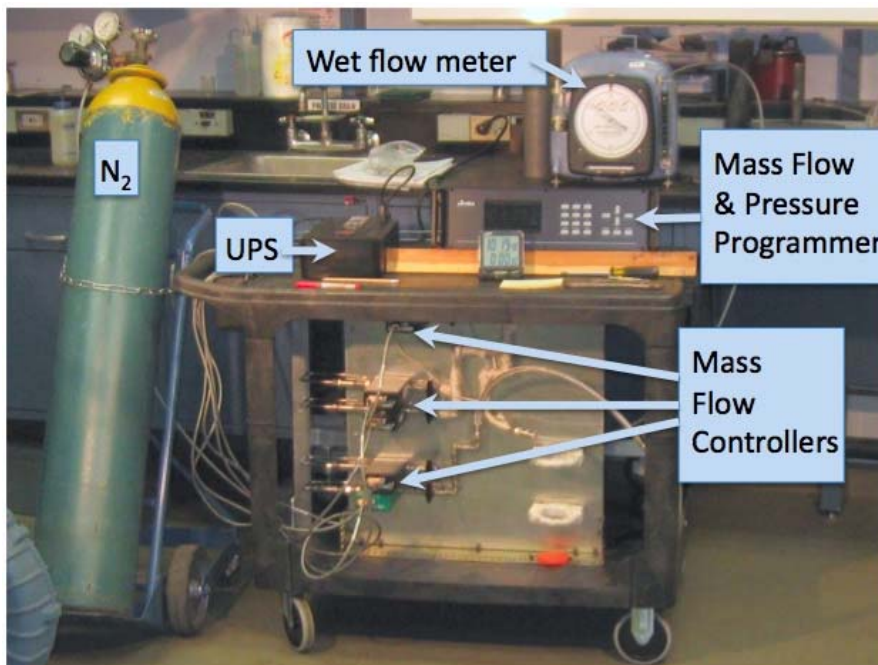


Figure 2- Portable manifold system undergoing mass flow controller calibration with a wet test meter.

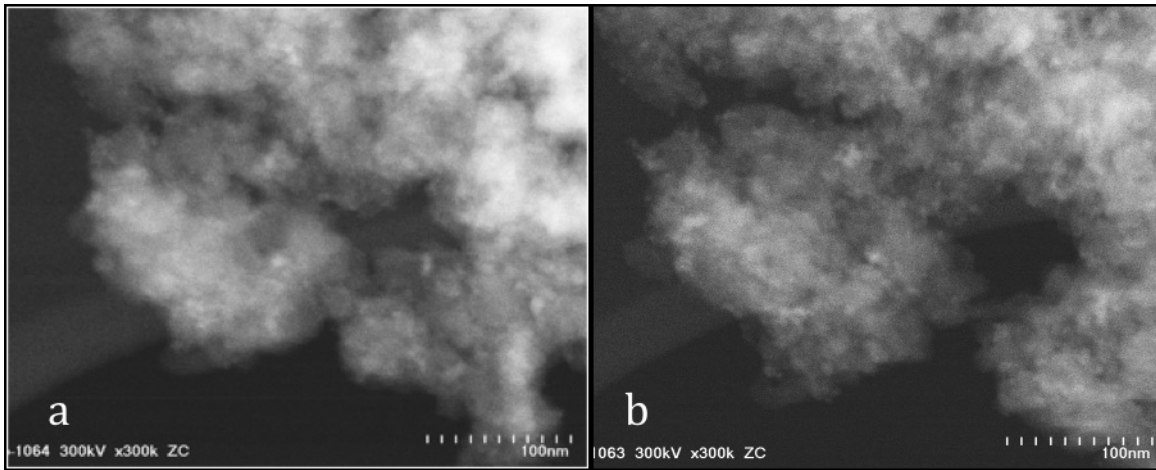


Figure 3- ADF images obtained a) before and b) after a scanning time of about 40 minutes.

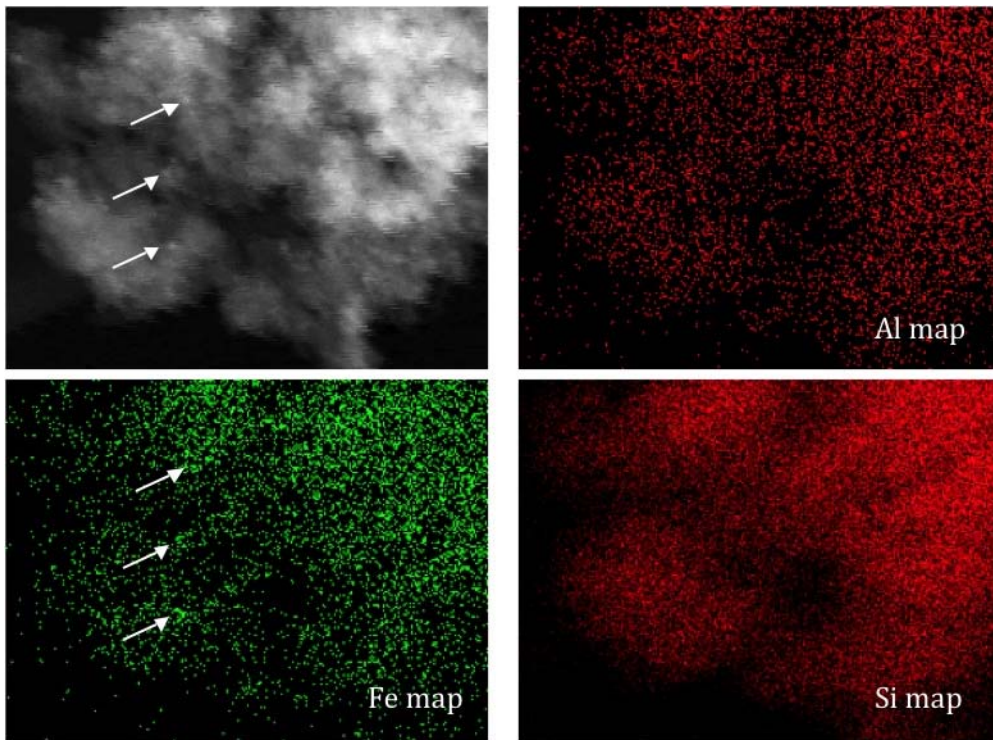


Figure 4- ADF image and corresponding X-ray images mapping out the Al, Fe and Si elements.



Figure 5- A new silicon drift x-ray detector, desired for inherently give low count rate environments, was installed on the ACEM.

# Agreement 10461: Durability and Reliability of Ceramic Substrates for Diesel Particulate Filters

Amit Shyam, Thomas R. Watkins and Edgar Lara-Curzio  
Oak Ridge National Laboratory

## Objectives/Scope

To develop/implement test methods to characterize the physical and mechanical properties of ceramic diesel particulate filters (DPFs), and to implement a probabilistic-based analysis to quantify their durability and reliability.

## Highlights

- ORNL participated in a round robin testing program to quantify the repeatability and reliability of a new ASTM test standard for honeycomb flexural testing.

## Technical Progress

In the reporting period, the ORNL team participated in an interlaboratory study (ILS) on flexure testing of commercially available honeycomb ceramics for applications such as diesel particulate filters. The ILS had the following stated objectives:

- Determine the repeatability and reproducibility for the new ASTM test method - ASTM C1674 -- Flexural Strength of Advanced Ceramics with Engineered Porosity (Honeycomb Cellular Channels) at Ambient Temperatures.
- Validate the honeycomb structure strength calculation and the linear cell count requirements in ASTM C1674.
- Determine the statistical distribution of flexure strength for the honeycomb ceramics, considering variations in test specimen size, materials, and architecture.

The following three compositions were tested as a part of the round robin testing program:

- 1) Cordierite material -- 300 cpsi/12 mil wall thickness
- 2) Cordierite material – 600 cpsi/4 mil wall thickness
- 3) Silicon Carbide material -- 300 cpsi/12 mil wall thickness

**Table 1:** Details of the five set of test specimens provided for the honeycomb flexural ILS.

Test Set	A	B	C	D	E
Composition	Cordierite	Cordierite	Cordierite	Silicon Carbide	Silicon Carbide
Cell Architecture (cps/wall mils)	300 /12	300 /12	600 /4	300 /12	300 /12
Test Method Geometry & Linear Cell Count for $d$ dimension	Method B – 9 cells	Method A – 15 cells	Method B – 12 cells	Method B – 9 cells	Method A - 15 cells
Specimen Size (mm)	13-25-116	22-25-150	13-25-116	13-25-116	22-25-175
Outer Test Span (mm)	90	130	90	90	130

The flexural specimens were cut and prepared by Cummins, and the details of the five test specimen geometries are included in Table 1. Two different outer loading spans of 130 mm (method A) and 90 mm (method B) were applied in the four point bend flexural tests. The failure loads and the corrected moment of inertia (MOI) calculations were utilized to calculate the nominal beam strength and wall fracture strength of the honeycomb. The strength values were calculated by application of a commercial reliability analysis software available at ORNL called Weibull++® 7. The materials for Test set E experienced crushing under the load points, and as such these values are not reported. The characteristic strength and Weibull modulus of data sets A-D (for both corrected and uncorrected MOI strength values) are summarized in Table 2.

**Table 2:** The two parameter Weibull analysis results for specimens from dataset A-D. The specimen with a Weibull modulus value greater than 50 indicates that Weibull analysis is not suitable for this dataset.

Data Set	Characteristic Strength (MPa)	Weibull Modulus
Flex A	2.09	31
Flex Corrected MOI A	5.13	24
Flex B	1.97	26
Flex Corrected MOI B	5.19	19
Flex C	2.79	35
Flex Corrected MOI C	7.57	>50
Flex D	8.43	21
Flex Corrected MOI D	19.68	17

It can be concluded from Table 2 that the SiC specimens (data set D) have higher strength values compared to the cordierite specimens (data set A-C) by a factor of 3 to 4. The effect of correcting for the moment of inertia of the honeycomb structure for data set A is shown in Figure 1. Whereas, the nominal beam characteristic strength for data set A is 2.09 MPa, the strength values corrected for the MOI leads to a wall characteristic strength of 5.13 MPa. It is recommended that analysis involving honeycombs should report the wall strength values since these are intrinsic to the material and not a function of the cell architecture.

The effect of specimen size on the Weibull parameters of honeycombs can be understood with the help of data presented in Figure 2. Even though two different sizes (and different outer spans) are represented in Figure 2, the characteristic strength of specimens from data set A and B are within ~ 1% of each other. This indicates that in the size range of specimens tested, there is no discernible size effect on the characteristic strength of the honeycomb specimens. The absence of a size effect may be a function of the multitude and uniformity of defects available to initiate cracks in the porous ceramic substrates. Detailed analysis of the results from all the labs in the ILS will be reported in the near future.

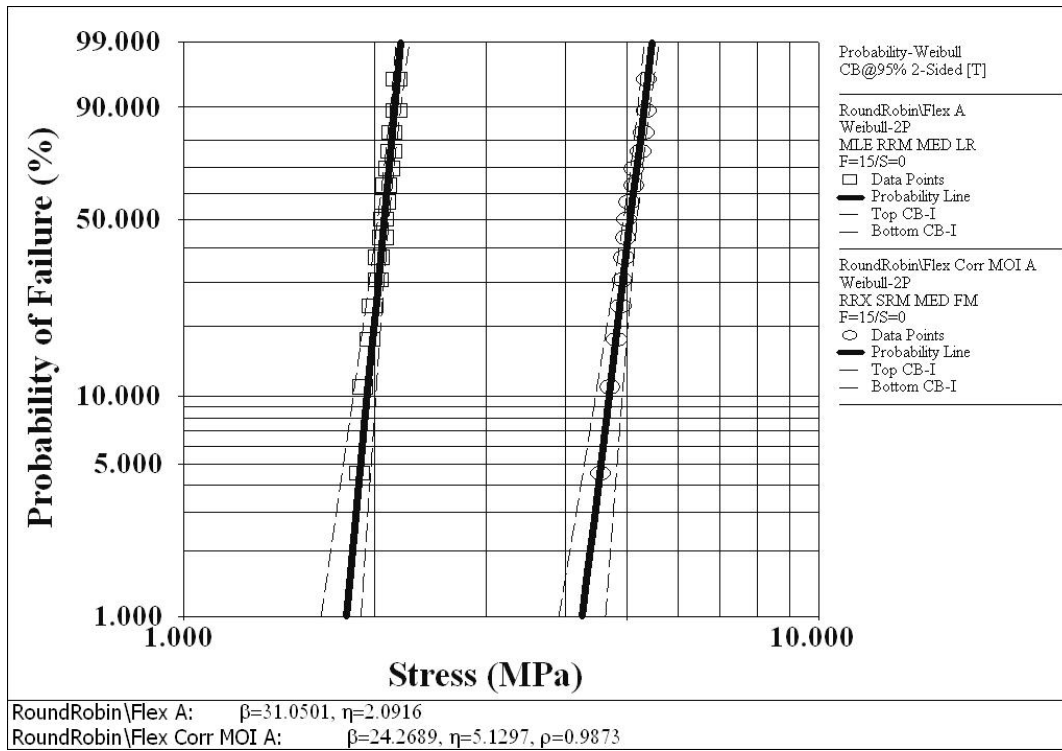


**Figure 1:** The effect of correcting for moment of inertia (right most data) on the Weibull parameters of a cordierite honeycomb specimen. Correcting for the wall architecture leads to computation of the wall strength of the honeycomb.

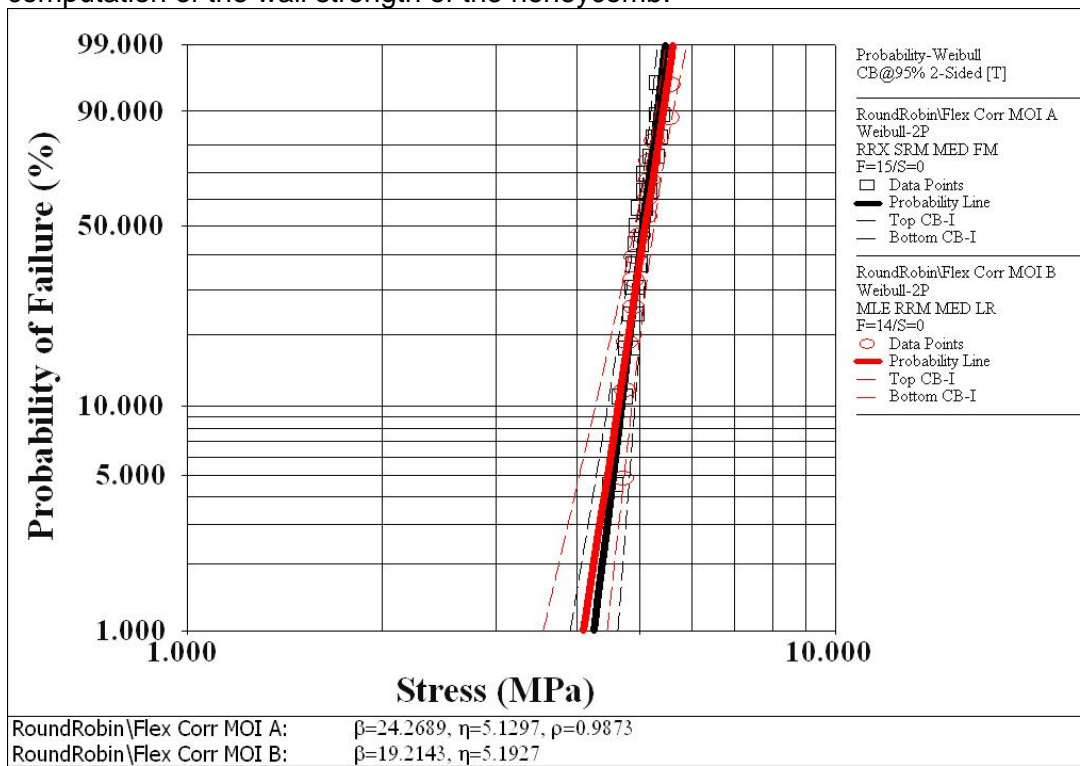


**Figure 2:** The effect of specimen size on the Weibull parameters of a cordierite honeycomb specimen. Larger specimens B (22-25-150 mm) are in red and the smaller specimens (13-25-116 mm) are in black.

## **Meetings**

ORNL personnel traveled to the Cummins Technical Center and met with Cummins personnel on Thursday November 13, 2008 and again on Thursday December 4, 2008 to discuss the technical progress and future plans of this CRADA.

## **Agreement 10635: Catalysis by First Principles - Can Theoretical Modeling and Experiments Play a Complimentary Role in Catalysis?**

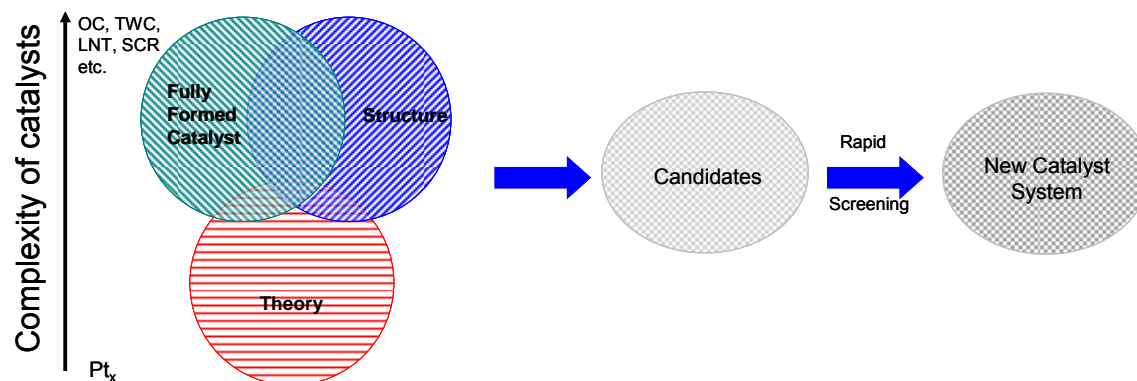
**C. Narula, M. Moses, L. Allard**  
**Oak Ridge National Laboratory**

### **Objective/Scope**

This research focuses on an integrated approach between computational modeling and experimental development, design and testing of new catalyst materials, that we believe will rapidly identify the key physiochemical parameters necessary for improving the catalytic efficiency of these materials. The results will have direct impact on the optimal design, performance, and durability of supported catalysts employed in emission treatment e.g. lean NO<sub>x</sub> catalyst, three-way catalysts, oxidation catalysts, and lean NO<sub>x</sub> traps etc.

The typical solid catalyst consists of nano-particles on porous supports. The development of new catalytic materials is still dominated by trial and error methods, even though the experimental and theoretical bases for their characterization have improved dramatically in recent years. Although it has been successful, the empirical development of catalytic materials is time consuming and expensive and brings no guarantees of success. Part of the difficulty is that most catalytic materials are highly non-uniform and complex, and most characterization methods provide only average structural data. Now, with improved capabilities for synthesis of nearly uniform catalysts, which offer the prospects of high selectivity as well as susceptibility to incisive characterization combined with state-of-the science characterization methods, including those that allow imaging of individual catalytic sites, we have compelling opportunity to markedly accelerate the advancement of the science and technology of catalysis.

Computational approaches, on the other hand, have been limited to examining processes and phenomena using models that had been much simplified in comparison to real materials. This limitation was mainly a consequence of limitations in computer hardware and in the development of sophisticated algorithms that are computationally efficient. In particular, experimental catalysis has not benefited from the recent advances in high performance computing that enables more realistic simulations (empirical and first-principles) of large ensemble atoms including the local environment of a catalyst site in heterogeneous catalysis. These types of simulations, when combined with incisive microscopic and spectroscopic characterization of catalysts, can lead to a much deeper understanding of the reaction chemistry that is difficult to decipher from experimental work alone.



Thus, a protocol to systematically find the optimum catalyst can be developed that combines the power of theory and experiment for atomistic design of catalytically active sites and can translate the fundamental insights gained directly to a complete catalyst system that can be technically deployed.

Although it is beyond doubt computationally challenging, the study of surface, nanometer-sized, metal clusters may be accomplished by merging state-of-the-art, density-functional-based, electronic-structure techniques and molecular-dynamic techniques. These techniques provide accurate energetics, force, and electronic information. Theoretical work must be based on electronic-structure methods, as opposed to more empirical-based techniques, so as to provide realistic energetics and direct electronic information.

A computationally complex system, in principle, will be a model of a simple catalyst that can be synthesized and evaluated in the laboratory. It is important to point out that such a system for experimentalist will be an idealized simple model catalyst system that will probably model a “real-world” catalyst. Thus it is conceivable that “computationally complex but experimentally simple” systems can be examined by both theoretical models and experimental work to forecast improvements in catalyst systems.

Our Goals are as follows:

- Our theoretical goal is to carry out the calculation and simulation of realistic supported Pt nanoparticle systems (i.e., those equivalent to experiment), in particular by addressing the issues of complex cluster geometries on local bonding effects that determine reactivity. As such, we expect in combination with experiment to identify relevant clusters, and to determine the electronic properties of these clusters.
- Our experimental goal is to synthesize metal carbonyl clusters, decarbonylated metal clusters, sub-nanometer metal particles, and metallic particles (~5 nm) on alumina (commercial high surface area, sol-gel processed, and mesoporous molecular sieve), characterize them employing modern techniques including Aberration Corrected Electron Microscope (ACEM), and evaluate their CO, NO<sub>x</sub>, and HC oxidation activity.
- This approach will allow us to identify the catalyst sites that are responsible for CO, NO<sub>x</sub>, and HC oxidation. We will then address support-cluster interaction and

design of new durable catalysts systems that can withstand the prolonged operations.

### **Technical Highlights**

Our results on experimental studies of Platinum-Alumina Systems and their nanostructural changes under CO-oxidation conditions are summarized in the following paragraphs. The results show how sample to sample variation can affect results. The effect of switching from gamma to theta alumina as a support material for the Pt particles is also illustrated.

Our early theoretical studies on gas phase unsupported clusters have been useful in developing the “catalyst by design” protocol. However, the results of theoretical studies on gas phase clusters can not be compared with experimental studies because the gas-phase cluster of 10 atoms exhibits chemistry almost approaching that of bulk metal particles. In view of this, we have initiated theoretical studies of supported clusters and their interaction with CO, NO<sub>x</sub>, and HC. We also summarize our theoretical studies.

### **Theoretical Studies**

We have selected  $\theta$ -alumina supported Pt clusters for theoretical studies because these clusters can be synthesized and the experimental results can be compared with theoretical results. While this is also true for  $\gamma$ -alumina and  $\alpha$ -alumina supported clusters, there are limitations of these supports. The structure  $\gamma$ -alumina remains to be conclusively determined preventing its theoretical examination.  $\alpha$ -Alumina, on the other hand, has practically not surface area and does not make a good support for catalyst.  $\theta$ -Alumina can be easily synthesized, exhibits a surface area of  $\sim 100 \text{ m}^2/\text{g}$ , and has a well-defined structure.

We have initiated our work by carrying out a density functional theoretical study of bulk  $\theta$ -alumina employing Vienna *ab initio* simulation package (VASP). Calculations were performed for generalized gradient approximation (CGA) of Perdew and Wang. The structure was fully relaxed with respect to volume as well as cell-internal and –external coordinates. Extensive test indicated that 600 eV was a sufficient cut-off to achieve highly accurate energy differences. The calculated cell parameters are as follows:  $a = 11.93$ ;  $b = 2.94$ ;  $c = 5.71$ ;  $\beta = 103.88$ ;  $V = 193.15$ . These data compare very well to experimental values of  $a = 11.85$ ;  $b = 2.904$ ;  $c = 5.622$ ;  $\beta = 103.8$ ;  $V = 187.8$ . The cell internal positions are as follows:

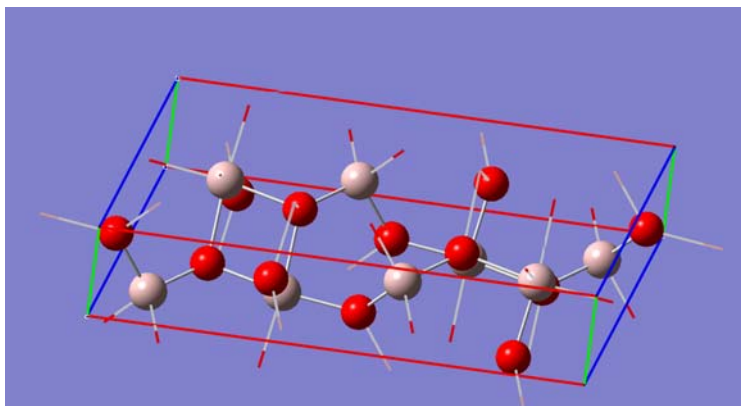


**Figure1:** Calculated Structure of  $\theta$ -Alumina

Calculated: Al1 (0.909, 0.204), Al2 (0.658, 0.317), O1 (0.160, 0.109), O2 (0.495, 0.257), O3 (0.826, 0.434)

Experimental: Al1 (0.917, 0.207), Al2 (0.660, 0.316), O1 (0.161, 0.098), O2 (0.495, 0.253), O3 (0.827, 0.427)

Thus, VASP has provided very accurate calculation of bulk  $\theta$ -alumina. Our next step is to calculate the structure of  $\theta$ -alumina surface and study its hydrolysis reaction before exploring the structure of Pt-clusters on  $\theta$ -alumina.

### **Experimental Studies**

CO Oxidation: 1nm 2%Pt/Al<sub>2</sub>O<sub>3</sub> catalyst, prepared by the traditional impregnation method from H<sub>2</sub>PtCl<sub>6</sub> • xH<sub>2</sub>O, were exposed to CO oxidation conditions. Previously reported batch studies of both 2%Pt/ $\gamma$ -Al<sub>2</sub>O<sub>3</sub> and 2%Pt/ $\theta$ -Al<sub>2</sub>O<sub>3</sub> samples were tested on a bench-top reactor under CO oxidation condition, 5%CO, 5%O<sub>2</sub> and 90%N<sub>2</sub>. The batch testing studies included testing two samples of each catalyst for CO oxidation efficiency as a function of temperature. Testing of one sample was stopped after oxidation was initiated and the Pt particles were imaged by scanning transmission electron microscope (STEM). The second samples were allowed to achieve quantitative CO oxidation before cooling to room temperature and repeating for a total of 3 cycles before imaging the particles by STEM. Temperature profiles for both catalysts ( $\gamma$  and  $\theta$ ) were identical after 3 cycles, initiating at 180°C and reaching quantitative conversion at 210°C.

While batch testing provides valuable data regarding conditions necessary for CO oxidation, nanostructural changes of the Pt particles observed after these tests are subject to sample-to-sample variation. In order to get a better understanding of how the nanostructures of certain particles change during CO oxidation, *ex-situ* reactor studies were carried out. The *ex-situ* reactor allows the exact same area of alumina to be imaged under each condition noted during the batch reactor tests. Figure 1 shows the exact same area from the 2%Pt/ $\gamma$ -Al<sub>2</sub>O<sub>3</sub> catalyst as a fresh sample, after it was exposed to initiation conditions (180°C) and after exposure to 3 cycles of quantitative CO oxidation conditions (210°C).

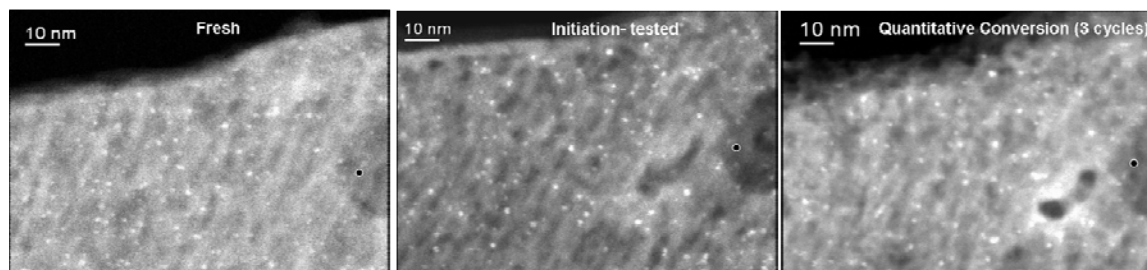


**Figure 2:** DF-STEM images of 2%Pt/ $\gamma$ -Al<sub>2</sub>O<sub>3</sub> fresh (left), the exact same area after initiation conditions, 180°C (middle), and again after 3 cycles of quantitative CO oxidation conditions, 210°C (right). The black circles rimmed in white are used to show the same spot in each image.

Visual inspection of the images in Figure 2 suggests some particle growth after exposure to CO oxidation condition compared to the fresh sample. A graphical program designed for measuring particle sizes of images obtained by electron microscopy was used to quantitatively evaluate the changes in the Pt particles nanostructure. Figure 3 shows the changes in particles size distribution for multiple areas followed on a 2%Pt/ $\gamma$ -Al<sub>2</sub>O<sub>3</sub> catalyst sample throughout the CO oxidization *ex-situ* study described above. The distribution curves show that while the average particle size changes little throughout the *ex-situ* study and the size range increases only slightly after both the initiation-testing and quantitative conversion cycles, the quantity of particles towards the higher end of the size range begins to increase. When compared to the results obtained by batch testing, the effect of sample-to-sample variation can be seen.

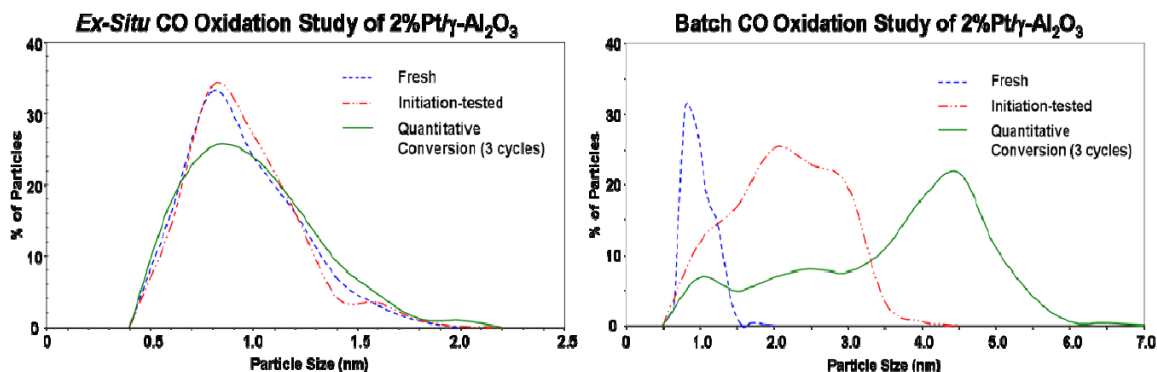


**Figure 3:** Pt particle size distribution curves obtained from STEM images of 2%Pt/ $\gamma$ -Al<sub>2</sub>O<sub>3</sub> taken in the course of an *ex-situ* reactor study (left) and a batch reactor study (right) under CO oxidation conditions.

A similar batch/*ex-situ* set of studies was also done for the 2%Pt/ $\theta$ -Al<sub>2</sub>O<sub>3</sub> catalysts to show any effect the catalysts' substrate morphology would have on nanostructural changes. Figure 3 shows the exact same area from the 2%Pt/ $\theta$ -Al<sub>2</sub>O<sub>3</sub> catalyst as a fresh sample, after it was exposed to initiation conditions (180°C) and after exposure to 3 cycles of quantitative CO oxidation conditions (210°C).

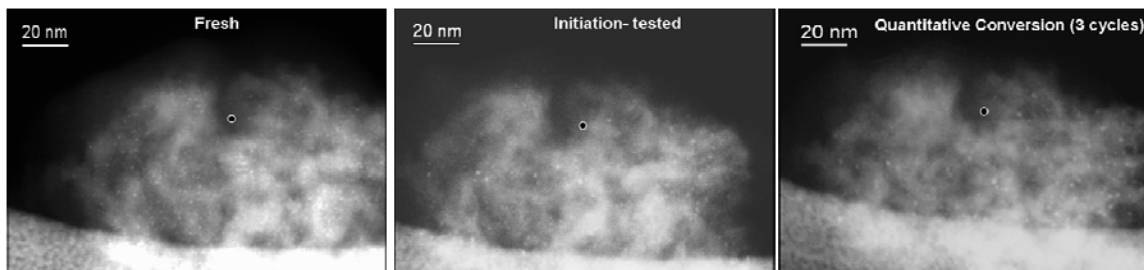


**Figure 4:** DF-STEM images of 2%Pt/ $\theta$ -Al<sub>2</sub>O<sub>3</sub> fresh (left), the exact same area after initiation conditions, 180°C (middle), and again after 3 cycles of quantitative CO oxidation conditions, 210°C (right). The black circles rimmed in white are used to show the same spot in each image.

Visual inspection of the images in Figure 4 suggests some particle growth after exposure to CO oxidation condition compared to the fresh sample. Figure 5 shows the quantitative changes in the particles size distribution for multiple areas followed on the 2%Pt/ $\theta$ -Al<sub>2</sub>O<sub>3</sub> catalyst sample throughout the CO oxidization *ex-situ*. The distribution curves show that while the bulk of the particles show little change in size throughout the *ex-situ* study, the size range increases after both the initiation-testing and quantitative conversion cycles.

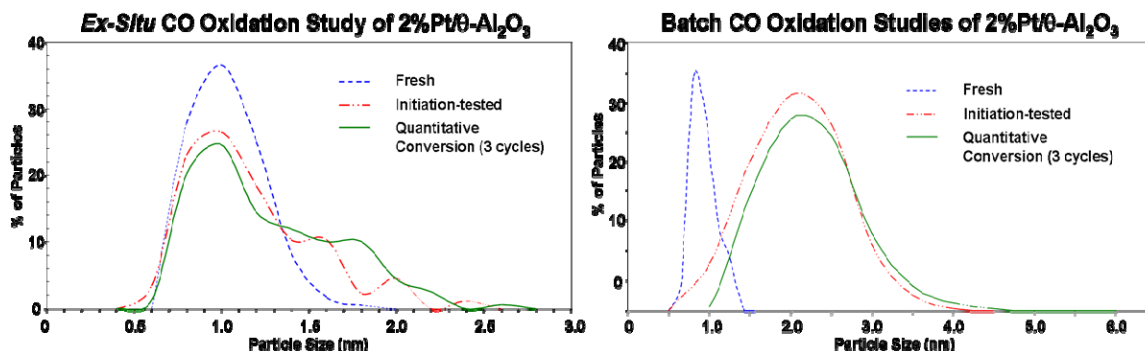


**Figure 5:** Pt particle size distribution curves obtained from STEM images taken in the course of an *ex-situ* reactor study (left) and a batch reactor study (right) under CO oxidation conditions.

**Table 1:** Average and median particle sizes obtained from multiple areas imaged by STEM for each catalyst 2%Pt/ $\gamma$ -Al<sub>2</sub>O<sub>3</sub> (*gamma*) and 2%Pt/ $\theta$ -Al<sub>2</sub>O<sub>3</sub> (*theta*). The exact same areas of the catalyst were imaged for the Fresh, Initiation-tested, and after 3 cycles of quantitative conversion (100% oxidation).

Support	Average (nm)		Median (nm)		Size Range (nm)	
	<i>gamma</i>	<i>theta</i>	<i>gamma</i>	<i>theta</i>	<i>gamma</i>	<i>theta</i>
<b>Fresh</b>	0.9	0.9	0.8	0.9	0.4 - 1.8	0.6 - 1.6
<b>Initiation-tested</b>	0.9	1.1	0.8	1.0	0.5 - 1.8	0.5 - 2.3
<b>3 cycles 100% Oxidation</b>	0.9	1.2	0.9	1.1	0.4 - 2.0	0.6 - 2.5

Table 1 compares the changes in particles size throughout the *ex-situ* studies of both catalysts. While the catalyst supported on  $\gamma$ -Al<sub>2</sub>O<sub>3</sub> shows little change in the Pt nanostructure, the platinum supported on  $\theta$ -Al<sub>2</sub>O<sub>3</sub> shows continued growth. The nanostructural stability is one of the major reasons that  $\gamma$ -Al<sub>2</sub>O<sub>3</sub> rather than  $\theta$ -Al<sub>2</sub>O<sub>3</sub> is used as the primary support component used in diesel emission catalyst.

**Next Steps:** We plan to carry out the following tasks:

- We will carry out selective catalytic reduction of diesel emissions on catalyst and monitor nanostructural changes in catalyst samples.
- Theoretical calculations will be carried out on a super cell of  $\theta$ -Al<sub>2</sub>O<sub>3</sub> and its interaction with water to understand the surface structure. Next, we will also study the Pt clusters supported on this structure.

### **Other Activities**

A joint project on lean NO<sub>x</sub> treatment is on going with John Deere Co under work for others arrangement.

### **Communication/Visitors/Travel**

M. DeBusk will be presenting an invited paper on "Catalyst by design: Combining the power of theory, experiments, and nanostructural characterization for catalyst development" at the American Chemical Society Meeting, March 22-27, Salt Lake City, Utah.

C.K. Narula is co-organizing a symposium on Catalysis at American Chemical Society Meeting, March 22-27, Salt Lake City, Utah.

### **Publications**

1. C.K. Narula, "Catalyst by Design – Bridging the Gap between Theory and Experiments at Nanoscale Level" Encyclopedia of Nanoscience and Nanotechnology, Vol. II, Taylor & Francis, New York, 2008, pp 771-782 (invited).
2. C.K. Narula, L.F. Allard, D.A. Blom, M. Moses-DeBusk, "Bridging the Gap between Theory and Experiments – Nano-structural Changes in Supported Catalysts under Operating Conditions" SAE-2008-01-0416.
3. C.K. Narula, L.F. Allard, D.A. Blom, M.J. Moses, W. Shelton, W. Schneider, Y. Xu, "Catalysis by Design - Theoretical and Experimental Studies of Model Catalysts", SAE-2007-01-1018 (invited).
4. C.K. Narula, M.J. Moses, L.F. Allard, "Analysis of Microstructural Changes in Lean NO<sub>x</sub> Trap Material Isolates Parameters Responsible for Activity Deterioration" SAE 2006-01-3420.
5. Y. Xu, W.A. Shelton, and W.F. Schneider, "The thermodynamic equilibrium compositions, structures, and reaction energies of Pt<sub>x</sub>O<sub>y</sub> (x = 1-3) clusters predicted from first principles," *Journal of Physical Chemistry B*, 110 (2006) 16591.
6. Y. Xu, W. A. Shelton, and W. F. Schneider, "Effect of particle size on the oxidizability of platinum clusters," *Journal of Physical Chemistry A*, 110 (2006) 5839.
7. C.K. Narula, S. Daw, J. Hoard, T. Hammer, "Materials Issues Related to Catalysts for Treatment of Diesel Exhaust," *Int. J. Amer. Ceram. Tech.*, 2 (2005) 452 (invited).

### **Presentations (last 12 months)**

1. Moses-DeBusk, M.; Narula, C.K. "Catalyst by design: Combining the power of theory, experiments, and nanostructural characterization for catalyst development," 227<sup>th</sup> National American Chemical Society Meeting, March 2009 (invited).
2. Narula, C.K.; Allard, L.F.; Blom, D.A.; Moses-DeBusk, M.; "Bridging the Gap between Theory and Experiments – Nanostructural Changes in Supported Catalysts under Operating Conditions", Society of Automotive Engineers – World Congress, April 2008 (invited).
3. Narula, C.K.; Moses, M.J.; Xu, Y.; Blom, D.A.; Allard, L.F.; Shelton, W.A.; Schneider, W.F.; 'Catalysis by Design – Theoretical and Experimental Studies of Model

Catalysts', Nanomaterials for Automotive Applications, Society of Automotive Engineers – international Congress, March 2007 (invited).

4. Blom, D.; Allard, L.; Narula, C.; Moses, M.; "Aberration-Corrected STEM ex-situ Studies of Catalysts" Wednesday, Microscopy and Microanalysis Meeting, 2007, August 5-9, Ft. Lauderdale, Florida. (Invited).
5. Narula, C.K.; Moses, M.J.; Blom, D.A.; Allard, L.F.; 'Catalysis by Design – Bridging the Gap Between Theory and Experiments– DEER 2007, Detroit, MI
6. Allard, L.F.; Blom, D.A.; Narula, C.K.; Bradley, S.; Catalyst Characterization via Aberration-Corrected STEM Imaging, 20th North American Catalysis Society Meeting, Houston, TX, June 17-22, 2007
7. Blom, D.A.; Moses, M.; Narula, C.K.; Allard, L.F.; Aberration-Corrected STEM Imaging of Ag/Al<sub>2</sub>O<sub>3</sub> Lean NO<sub>x</sub> Catalyst, 20th North American Catalysis Society Meeting, Houston, TX, June 17-22, 2007
8. Narula, C.K.; Moses, M.; Blom, D.A.; Allard, L.F.; Nano-structural Changes in Supported Pt Catalysts during CO oxidation, 20th North American Catalysis Society Meeting, Houston, TX, June 17-22, 2007
9. Moses, M.; Narula, C.K., Blom, D.A.; Allard, L.F.; Ex-situ Reactor Enabled Microstructural Monitoring: Elucidating Lean NO<sub>x</sub> Trap Deterioration Parameters, 20th North American Catalysis Society Meeting, Houston, TX, June 17-22, 2007

## **Agreement 9105: Ultra-High Resolution Electron Microscopy for Characterization of Catalyst Microstructures and De-activation Mechanisms**

**L.F. Allard, C.K. Narula  
Oak Ridge National Laboratory**

**L. Germinario  
Eastman Chemical Co.**

### **Objective/Scope**

The objective of the research is to characterize the microstructures of catalyst materials of interest for the treatment of NO<sub>x</sub> emissions in diesel and lean-burn gasoline engine exhaust systems. The research heavily utilizes new capabilities and techniques for ultra-high resolution transmission electron microscopy with the HTML's aberration-corrected electron microscope (ACEM). The research is focused on understanding the effects of reaction conditions on the changes in morphology of heavy metal species on "real" catalyst support materials (typically oxides), and the understanding of the structures of model mono-, bi- and multi-metallic catalyst systems of known particle composition. With the former systems, these changes are being studied utilizing samples treated in both steady-state bench reactors and a special *ex-situ* catalyst reactor system especially constructed to allow appropriate control of the reaction. Model samples of nanoparticulates of controlled composition on carbon or oxide supports are also being studied in collaboration with the catalysis group at the University of Texas-Austin (Profs. M. Jose-Yacaman and P. Ferreira). Studies of the behavior of Pt species on oxide substrates are also being conducted with Drs. S. A. Bradley of UOP Co., and C. H. F. Peden of PNNL. NO<sub>x</sub> trap catalyst materials BaO/Al<sub>2</sub>O<sub>3</sub> are being studied with Dr. Peden and Dr. Ja Hun Kwak at PNNL.

### **Technical Progress**

#### **In-Situ Microscopy Developments**

"Air-lock" Reaction Capability: As an adjunct capability to our current development of an "environmental cell" holder for our JEOL 2200FS aberration-corrected STEM/TEM instrument ("ACEM"), we have fabricated and installed a new manifold system on the microscope that give us a unique capability for reaction studies using the Protochips Aduro™ heater chip technology reported in the last few quarterlies. A brief reminder: we are working with Protochips Co. (Raleigh, NC) on developing a MEMS-based heater chip technology which allows e.g. catalyst TEM samples to be heated up to 1200°C in 1 millisecond (and cooled just as quickly). This remarkable performance is combined with a very high stability, so that ultra-high resolution images can be recorded in high-angle annular dark-field mode, with sub-Ångström resolution. This heater chip technology also forms the basis for the environmental cell, to be reported in detail next quarter. However, in the e-cell, we expect only to be able to conduct reactions at gas pressures

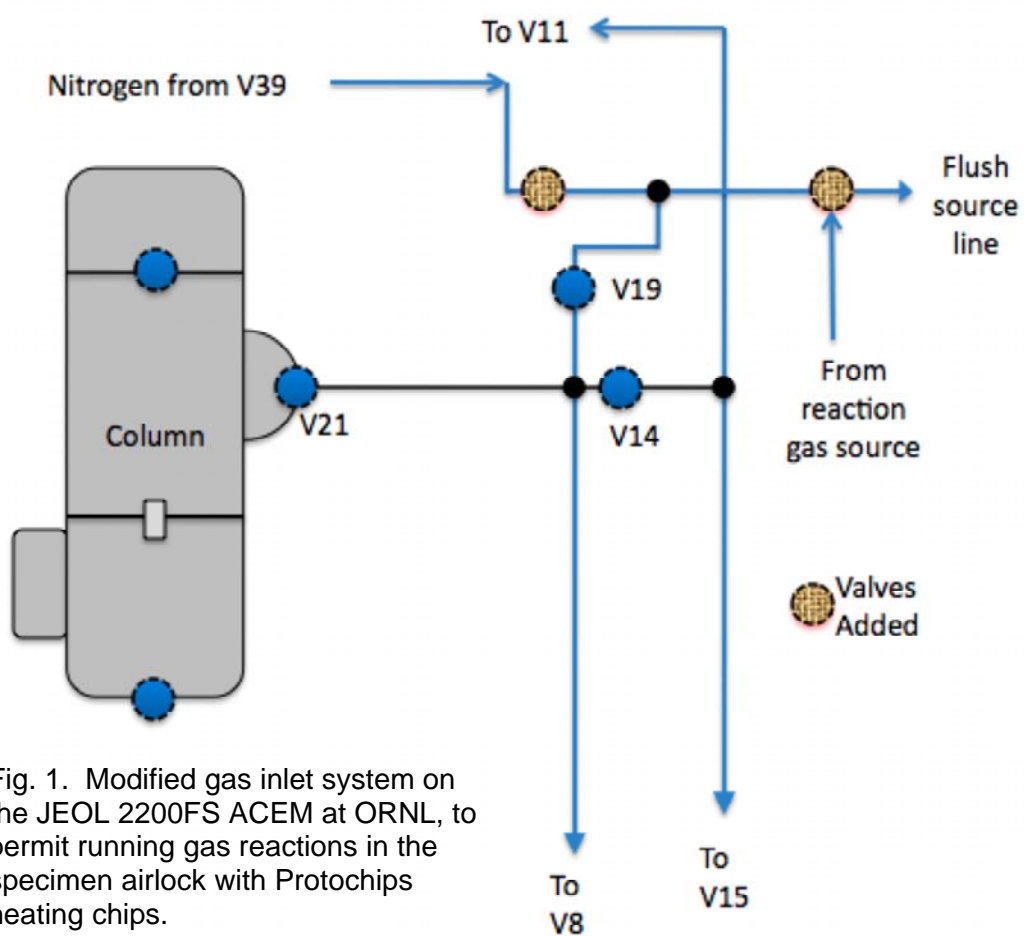


Fig. 1. Modified gas inlet system on the JEOL 2200FS ACEM at ORNL, to permit running gas reactions in the specimen airlock with Protochips heating chips.

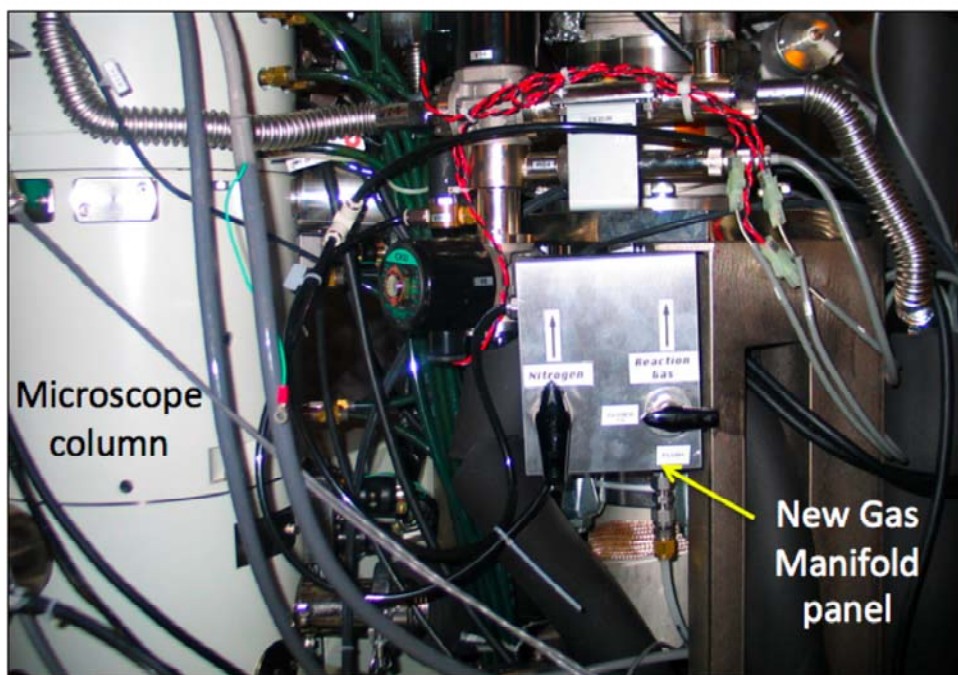


Fig. 2. New gas manifold for airlock reaction gas control installed on ACEM.

of 20 Torr or less, while it is of interest to also do reaction studies at atmospheric pressure in some cases. The “airlock” reaction system provides this capability. Figure 1 shows a schematic diagram of the modification we made in the microscope’s airlock pumping line to allow control of the gas into the airlock. Figure 2 shows the valve panel added to allow manual control of the reaction process. Since we have to install and retract the specimen holder by hand (not everything on our microscope can be remotely operated!), we felt it was not necessary to fit the manifold with solenoid valves. Figure 3 shows the setup for an airlock reaction, with the close juxtaposition of the valve manifold and heater holder inside the airlock evident.

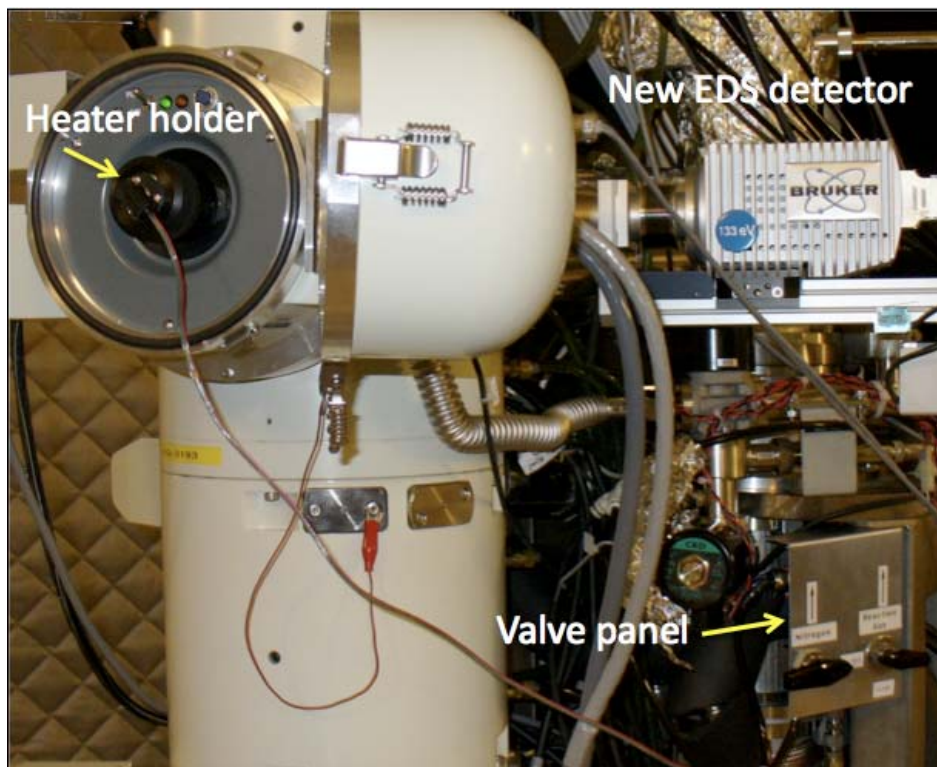


Fig. 3. View of JEOL 2200FS column with Protochips holder installed (note electrical lead), valve panel for airlock reaction gas control, and also new “silicon-drift” energy dispersive X-ray detector, on consignment.

The basic idea of the airlock reactor is that, because the Protochips heater can be cycled from room temperature to an elevated temperature and back essentially instantaneously, we can study reactions at atmospheric pressure by first imaging a sample area of interest at RT in the microscope (when electron beam effects are minimized), then, after storing the sample position electronically, we can retract the holder into the sample airlock, and admit a desired reaction gas. The gas is cycled to atmospheric pressure several times to purge the chamber, then the sample is heated to a desired temperature for a desired time, and cooled instantaneously. By simply pumping out the airlock, the sample is re-inserted into the column, the original position recovered, and images of the same area after reaction are recorded. This procedure can be cycled a number of times in a single observation session, because of the

simplicity of the process. It should be noted that this new procedure basically replaces (for some reactions at least) our older “ex-situ” reactor system, with which we had to remove the specimen rod entirely from the microscope column, transport it to the reactor, extract the sample from the holder when it was inside the reactor, do a bulk heating experiment which required significant time to ramp up to temperature and back down to RT after the experiment, then reverse the process to get the sample back into the microscope. Disadvantages of this process included the difficulty of keeping the sample protected from the atmosphere in the case of air-sensitive catalysts, and the problems with re-locating the original sample areas, along with the time-consuming process compared to our new technique.

Early work using the Protochips heater system and the airlock reaction capability has been conducted in our collaboration with Dr. Louis Germinario of Eastman Chemicals Co. (Kingsport, TN). We are studying the behavior of catalytic materials such as palladium on alumina and ruthenium on carbon in order to better understand the phenomena associated with electron beam heating effects versus thermal treatment using our heating holder technology, and these materials are convenient, commercially available catalysts. An example of the results of a reduction experiment on nanoparticles of Pd on alumina is shown in Fig. 4. The Pd particles in this catalyst were often observed to have an apparent amorphous external coating or shell, around all or

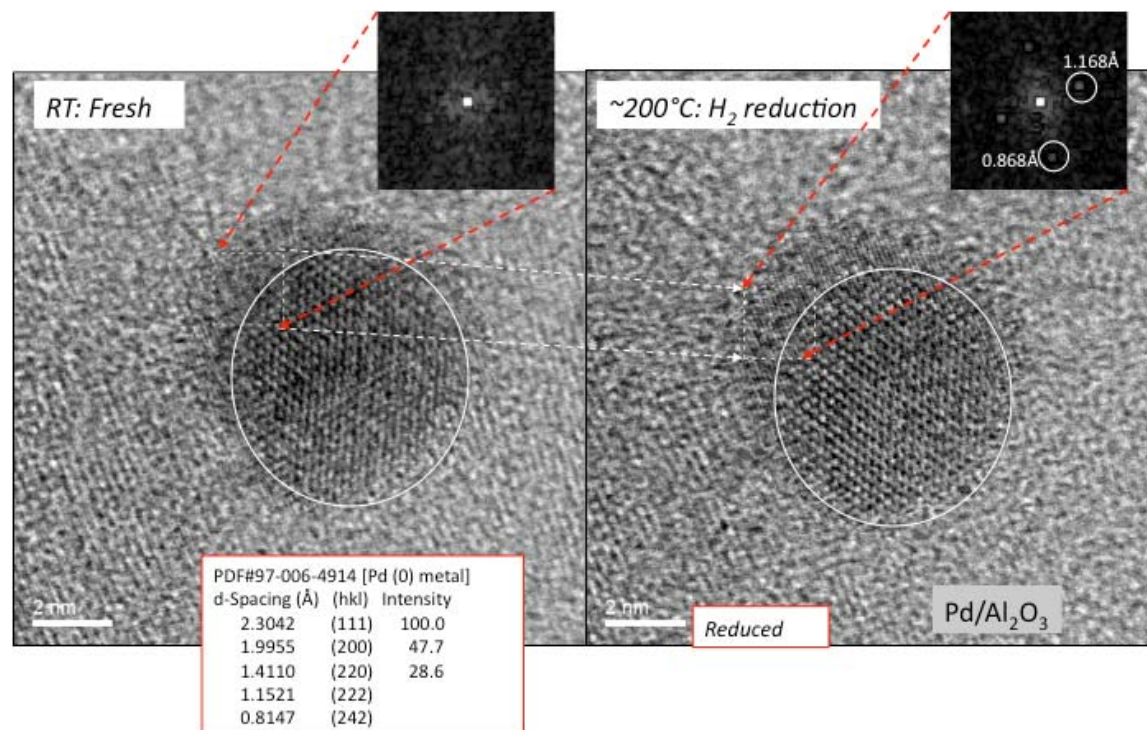


Fig. 4. Pd nanoparticle on alumina support, before (left) and after (right) airlock reduction at 200°C. Amorphous component at surface shows crystalline lattice after reduction treatment.

part of a metallic particle. The amorphous shell was expected to be PdO, which should reduce to the pure metal when exposed to a reducing gas (in this case, 4% H<sub>2</sub> in N<sub>2</sub>), at slightly elevated temperatures. The bright field image before and after reduction in the

specimen airlock for 10 minutes is shown in the figure, since the crystal lattice is often more easily visible in BF vs. dark field images. A computed diffractogram from the apparent amorphous area is shown inset in Fig. 4a, and a similar diffractogram is shown in Fig. 4b, which now has two discrete periodicities showing. The lattice structure in the prior amorphous region is also clearly visible in the image, and the 1.168Å spacing associated with this lattice is consistent with the 222 lattice plane spacing of Pd, as indicated. This is the predominant spacing seen in the image, and suggests strongly that the reduction has proceeded towards metallic Pd.

**Progress on the Second-Generation E-Cell Holder:** The first prototype environmental cell holder we developed with Protochips Co. was described in the annual report. That holder proved to be unacceptable for use in our ACEM, because it was too thick to be used practically on a routine basis. The design employed an upper thin film window and a lower thin film window, sandwiched around a heater chip on which the catalyst powder sample could be dispersed. This resulted in a design that was 1.7mm thick, which barely fit into the 2mm gap of our objective lens pole piece. The new holder, which has been designed, is a “two-window” device, with the upper window being a heater chip that would have the catalyst sample dispersed on the interior side, between the heater membrane and a lower thin film window. Initial drawings show that the new device, which will also have gas In and Out orifices for supply and return of reaction gases, can be fabricated to be less than 1.4mm, a thickness which is much more compatible with the very narrow gap of the pole piece. Tests of the second-generation holder will be reported in the next quarterly.

**Heater Holder for Hitachi HF-3300 TEM/STEM:** A new holder for the Hitachi 300kV cold field-emitter TEM/STEM instrument has been constructed, to provide the capability to do heating experiments similar to those being conducted in the ACEM, but which will also allow X-ray analysis with high detection sensitivity as well as electron holography to be performed on samples at elevated temperatures. Figure 5 shows this holder, with a Protochips heater device installed and heated to ~1000°C. Initial tests on this new holder are commencing.

**PNNL NO<sub>x</sub> trap research collaboration:** we completed microscopy on samples of BaO-Al<sub>2</sub>O<sub>3</sub> NO<sub>x</sub> trap materials for a study we have worked on with Drs. Ja Hun Kwak and C.H.F. Peden at PNNL. A publication (see below) was submitted to the Journal of Catalysis, and will be out first quarter 2009.

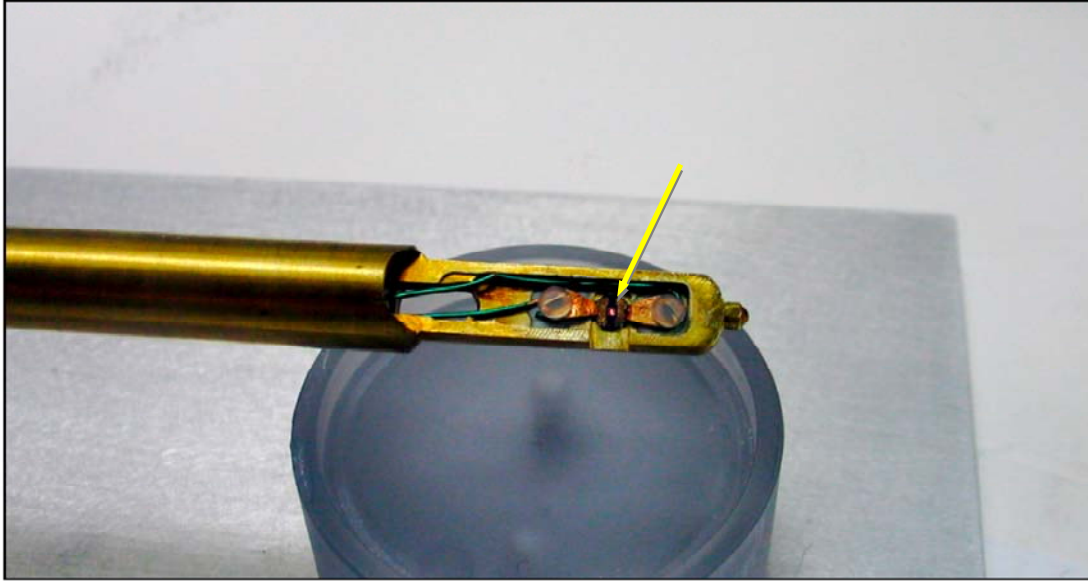


Fig. 5. Heater holder fabricated for new Hitachi HF-3300 300kV field-emission TEM/STEM instrument, showing heater device at  $\sim 1000^{\circ}\text{C}$  in air (arrowed).

## References

### Status of Milestones

On schedule

### Communications/Visits/Travel

L. F. Allard, et al., **Developments in Aberration-Corrected Imaging at Elevated Temperatures Using a New MEMS-Based Heating Technology**, ORNL-Hitachi Workshop on “Advanced Electron Microscopy in Materials Science,” Oak Ridge National Laboratory, November 2008

### Publications

**“Understanding the nature of surface nitrates in BaO/ $\gamma$ -Al<sub>2</sub>O<sub>3</sub> NO<sub>x</sub> storage materials: A combined experimental and theoretical study,”** Ja Hun Kwak, Donghai Mei, Cheol-Woo Yi, Do Heui Kim, Charles H.F. Peden, Lawrence F. Allard and János Szanyi, *Journal of Catalysis* (in press).

## **Agreement 17895: Durability of ACERT Engine Components**

**Hua-Tay Lin, T. Kirkland, and A. A. Wereszczak  
Oak Ridge National Laboratory**

**N. Philips and J. Jensen  
Caterpillar, Inc.**

### **Objective/Scope**

There are four primary goals of this research agreement, which contribute toward successful design and implementation of advanced lightweight material components to achieve high-efficiency engine of 55% of heavy-duty diesel engines by 2012 as set under the 21st CT program: 1) the generation of a mechanical engineering database of candidate advanced lightweight materials before and after exposure to simulated engine environments; 2) the microstructural evolution and accompanied chemical changes during service in these advanced materials; 3) material selection, development, and design of complex-shaped components, and 4) application and verification of probabilistic life prediction methodology for advanced high-efficiency diesel engine components. The methodology implemented would also help to manufacture consistent mechanical reliability and performance of complex shaped components.

### **Technical Highlights**

The objective of this subtask is to provide important material support to address multiple key barriers to enable the design of high-efficiency and clean heavy-duty diesel engines. There key technological barriers are 1) parasitic, friction, and heat transfer losses accounts for > 30% of the available energy in internal combustion engines, 2) High Efficiency Clean Combustion (HECC) peak pressures challenge structural limits of current materials and designs, and 3) improvements in thermal management will require the incorporation and evaluation of new materials concepts. This may lead to additional opportunities in managing exhaust energy. The materials technologies taken to address each barrier will be described as follows.

Reduction in heat rejection could be achieved by the application of durable, cost-effective thermal barrier coatings (TBCs) for piston and exhaust port, and exhaust manifold, and also development of advanced TBCs resistant to thermal cycling. The increase in waste heat recovery could be accomplished via 1) the enhancement of gear strength and wear resistance for turbocompounding, 2) development of light weight, high strength, and efficient heat exchanger materials, and 3) application of thermoelectric generation systems. Also, optimization of internal combustion engine can be achieved by 1) the application of lighter, corrosion resistant high-temperature valves, 2) enhanced fuel injector designs and materials, 3) high-strength cylinder heads and engine blocks, and 4) reduced heat rejection in cylinder head. In addition, the high-efficient aftertreatment (and thus NO<sub>x</sub> reduction) could be accomplished by the significant improvement in ceramic DPF properties and design and also the catalyst systems. The reduction in friction can be achieved by the development of low friction, durable liner/ring ceramic coatings and surfacing technology. Lastly, high engine efficiency and clean emission engine can be achieved by the employment of high

efficiency cooling systems via the development of advanced corrosion resistant resistance aluminum alloys and coatings and cost-effective stainless steels. These key supporting materials activities will be discussed and prioritized with the engine companies and will be reported in the next quarterly report.

#### **Status of FY 2009 Milestones**

Complete mechanical database and microstructure characterization of new components designed for ACERS diesel engine. **(09/09)** – On schedule.

#### **Communications/Visits/Travel**

Communications with Drs. Philip and Jensen at Caterpillar regarding the discussion of supporting materials for ACERS engine and components.

Communications with Dr. Kass at NTRC regarding the up-to-date status on the installation of ACERS engine.

#### **Problems Encountered**

None.

#### **Publications/Presentations/Awards**

None.

#### **References**

None

## Agreement 14957: High Temperature Thermoelectrics

A. A. Wereszczak, T. P. Kirkland, and H. Wang  
Oak Ridge National Laboratory

### **Objective/Scope**

Measure needed thermomechanical and thermophysical properties of candidate thermoelectric (TE) materials and then use their data with established probabilistic reliability and design models to optimally design automotive and heavy vehicle TE modules. Thermoelectric materials under candidacy for use in TE modules tend to be brittle, weak, and have a high coefficient of thermal expansion (CTE); therefore, they can be quite susceptible to mechanical failure when subjected to operational thermal gradients. A successfully designed TE module will be the result of the combination of temperature-dependent thermoelastic property and strength distribution data and the use of the method of probabilistic design developed for structural ceramics.

### **Technical Highlights**

#### *Strength Testing*

This quarterly report chronicles the comparison of the uncensored Weibull flexure strength distributions of n- and p-type bismuth telluride as a function of several variables (orientation, temperature, and how machined). Materials were purchased and cut to into shape by Marlow Industries, Inc., Dallas, TX. This thermoelectric material is mature and its testing will provide a reference database that can be used to compare developmental thermoelectric materials too. A large number of specimens enables the generation of statistically significant data. Uniaxial and biaxial flexure strength test methods will enable us to censor the data according to edge-type and surface-type, and perhaps even volume-type flaws.

There is transverse isotropy in bismuth telluride owing to the method it is fabricated. Therefore, uniaxial flexure (3-pt-bend) strength coupons were harvested in a manner to enable the study of strength-dependence on orientation. This was examined for both n- and p-type bismuth telluride. For both the n- and p-type, the RZ orientation was approximately twice that of the RR orientation as shown in Fig. 1. For the stronger RZ orientation, the strengths of the n- and p-type were equivalent though the former showed more scatter in its strength distribution. For the RR orientation, the n-type was slightly stronger than the p-type.

The effect of temperature was explored by testing uniaxial flexure specimens at room temperature and 225°C. Those results are illustrated in Fig. 2. Compared to room temperature, the strength decreased by approximately 15% at 225°C. This strength decrease occurred for both the n- and p-types and within both orientations for each.

The effect of surface preparation method on strength was examined. One pair of parallel surfaces were ground while the other pair was produced through a slicing process. The comparison of their strengths are shown in Fig. 3. There was not a

significant difference in their strengths though the strength distributions for the ground surfaces tended to exhibit more scatter. This trend was independent of the type and orientation.

The "potential" strength of the bismuth tellurides was explored by polishing some specimens and then measuring their strength. These results are shown in Fig. 4. Specimens of this geometry were only available for the p-type, so the n-type was not tested in this fashion. As expected, the biaxial flexure strength was higher for polished specimens, and these values (in reference to the effective area) provide a high end bound of the strength potential of this material.

#### *Transport Properties Testing*

Electrical conductivity and Seebeck coefficient of n-type materials were tested from room temperature to 250°C to understand the effect of orientation on heat and electric current flows. Three RZ, 2 mm x 2 mm x 15 mm, bars and three RR bars with similar dimensions were prepared. Measurements were conducted at 25°C steps. At each temperature, three differential temperatures were used to calculate Seebeck coefficient. As shown in Figs. 5 and 6, the electrical resistivity and Seebeck coefficient showed different behavior as a function of temperature. The results are similar to the p-type materials tested earlier in this project.

Six 1-mm-thick n-type plates in both RZ and RR directions were prepared for thermal transport measurements. Initial room temperature xenon flash diffusivity results showed about 30% difference between the RZ and RR samples. Higher temperature testing will be carried in the next quarter for complete ZT analysis of the n-type materials.

#### *Collaboration with Marlow*

The statement of work for a proposed CRADA with Marlow was modified during this present reporting period, and reinitiated for administration. It is anticipated that the CRADA could initiate at the end of the second quarter.

#### **Status of FY 2009 Milestones**

Generate thermoelastic and mechanical property database as a function of temperature on at least one candidate HTTE p- and n-type material fabricated by Marlow Industries.  
*On schedule.*

#### **Communications/Visits/Travel**

Numerous communications occurred between Wereszczak and Marlow's J. Sharp during the present reporting period.

#### **Problems Encountered**

None.

### Publications/Presentations/Awards

J. R. Salvador, J. Yang, X. Shi, H. Wang, and A. A. Wereszczak, "Transport and Mechanical Property Evaluation of  $(\text{AgSbTe}_2)_{1-x}(\text{GeTe})_x$  ( $x=0.8, 0.82, 0.85, 0.87$  and  $0.90$ )," in preparation and to be submitted to Scripta Materiala, 2009.

J. R. Salvador, J. Yang, X. Shi, H. Wang, A. A. Wereszczak, H. Kong, and C. Uher, "Transport and Mechanical Properties of Yb-Filled Skutterudites," in preparation and to be submitted to Acta Materiala, 2009.

### References

None.

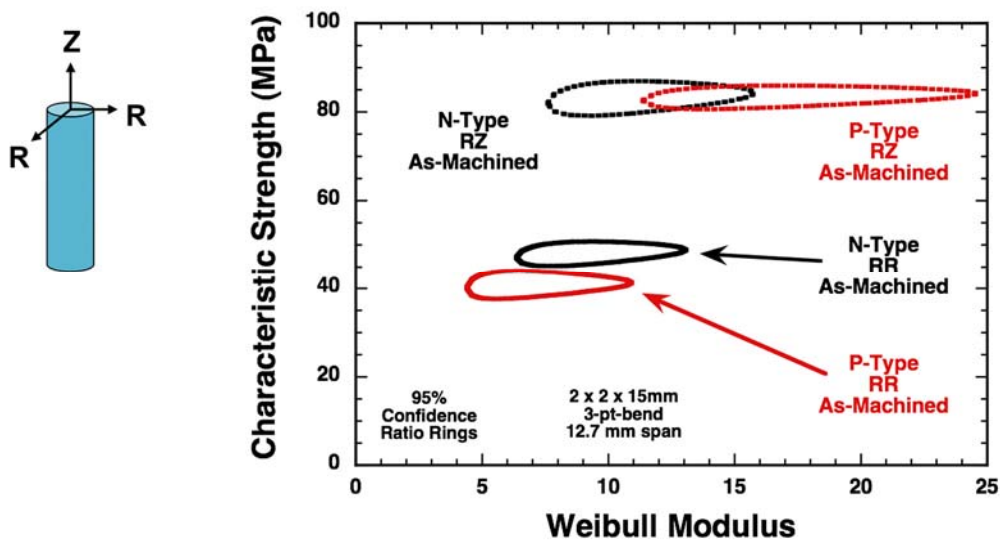


Figure 1. Weibull uniaxial flexure strength distributions for n- and p-type as a function of orientation at 25°C.

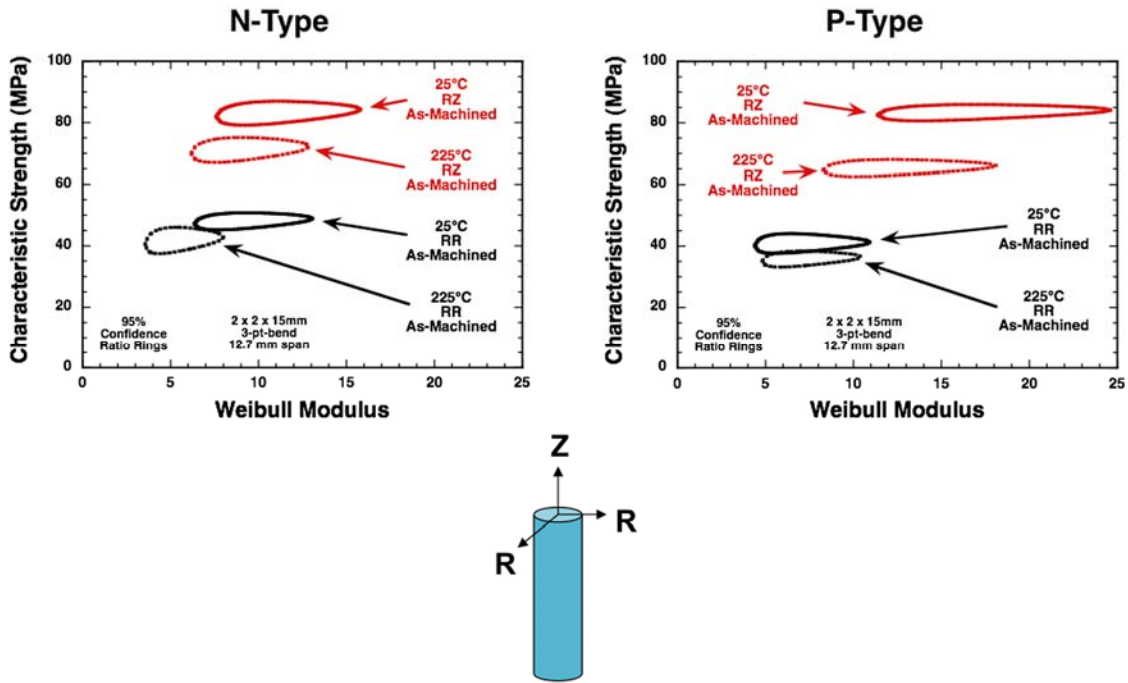


Figure 2. Weibull uniaxial flexure strength distributions for n- and p-type as a function of orientation and temperature.

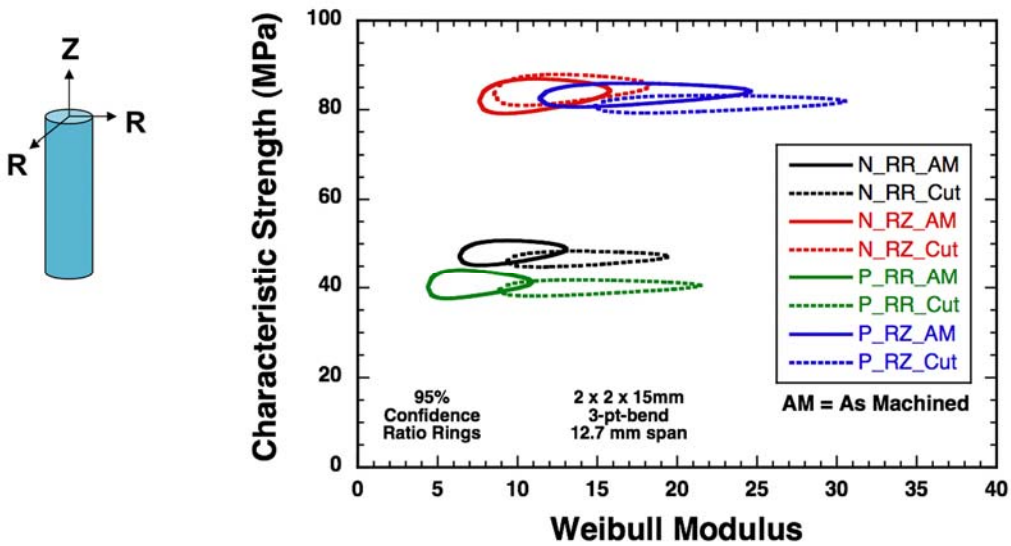


Figure 3. Weibull uniaxial flexure strength distributions for n- and p-type as a function of orientation and method of surface preparation at 25°C.

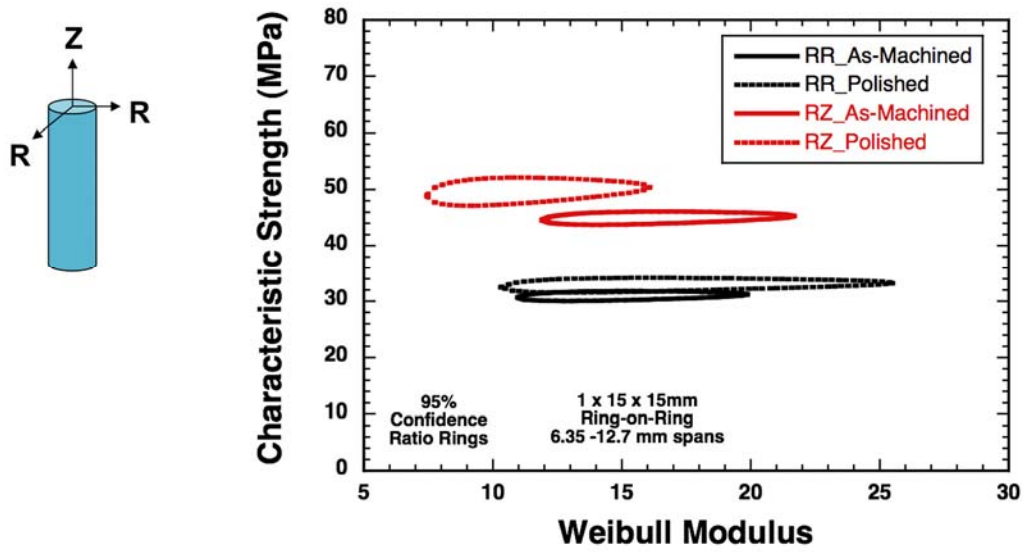


Figure 4. Weibull biaxial flexure strength distributions for p-type as a function of orientation and method of surface preparation at 25°C.

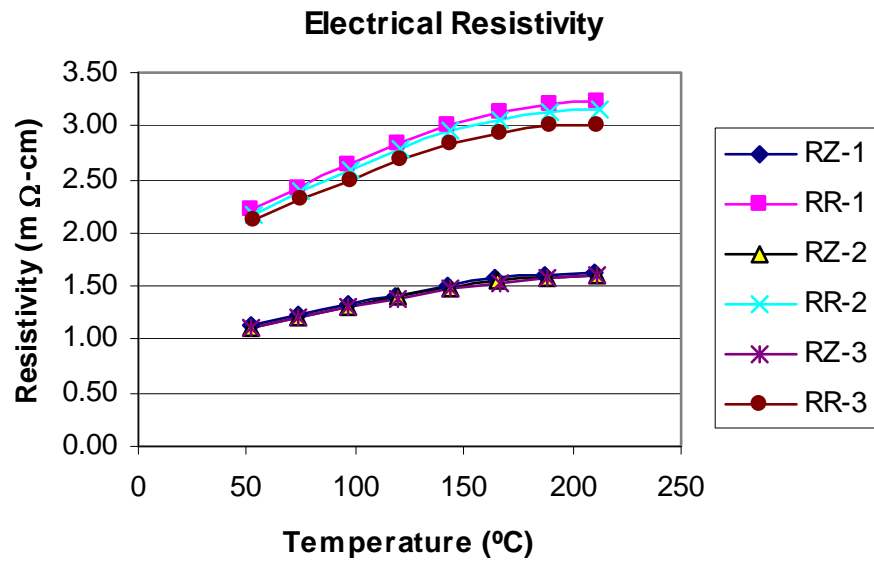


Figure 5. Electrical resistivity of N-type bars in the RR and RZ directions.

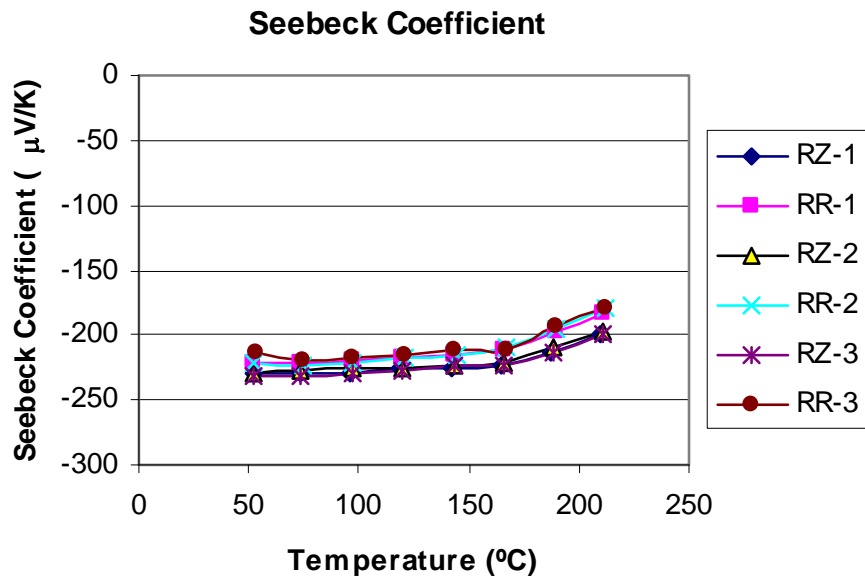


Figure 6. Seebeck Coefficient of N-type bars in the RR and RZ directions.

## Agreement 16308 – Science Based Approach to Thermoelectric Materials

David J. Singh  
Oak Ridge National Laboratory

### Objective/Scope

We will use modern science based materials design strategies to find ways to optimize existing thermoelectric materials and to discover new families of high performance thermoelectrics for waste heat recovery applications. The emphasis will be on the thermoelectric figure of merit at temperatures relevant to waste heat recovery and on other properties important for applications, especially anisotropy and mechanical properties.

### Technical Highlights

#### *Mn-Pnictides*

The primary focus of this effort is to identify materials that are of practical utility on vehicles. Therefore we are primarily interested in materials that are potentially low cost in volume and at the same time have adequate performance. At present two of the likely candidate materials: PbTe and the so-called LAST compounds (which are based on a heavily modified PbTe type phase) have large concentrations of Te. While there may be design strategies for reducing the amount of thermoelectric material in waste heat recovery systems, there is concern among automotive manufacturers about the practicality of wide spread deployment of a Te based technology. Although Te prices at present are affordable, the supply is Te is very limited, with production mainly as a by-product of copper production. This concern was mentioned in several of the presentations by manufacturers at the recent International Conference on Thermoelectricity in Oregon.

As such it is of interest to examine non-telluride thermoelectric phases. In this context, there was a recent report from China (H.F. Wang, et al., Journal of Alloys and Compounds, 2008) on the characterization of ThCr<sub>2</sub>Si<sub>2</sub> structure BaMn<sub>2</sub>Sb<sub>2</sub> as a thermoelectric material. It was reported that the material shows high thermopowers at room temperature, but insufficient carrier mobility. Doping studies were not reported making it very difficult to assess the potential of this phase. The phase is related to arsenides in the same structure based on Fe and Co that have high conductivity, and also relatively high thermopower. Based on this we used first principles calculations to calculate properties of BaMn<sub>2</sub>Sb<sub>2</sub> and also the arsenide BaMn<sub>2</sub>As<sub>2</sub>. The goals were to understand the reported results in BaMn<sub>2</sub>Sb<sub>2</sub> and assess whether doping studies were warranted, and also to determine if the arsenide would have better properties, especially considering the much better conduction of the arsenide Fe, Co and Ni phases. In addition to the theoretical calculations, we collaborated with A.S. Sefat (an ORNL Wigner fellow in the correlated electron materials group), who grew a single crystal of BaMn<sub>2</sub>As<sub>2</sub> and performed electrical transport and specific heat measurements to validate our calculations.

Some of the results of our study on BaMn<sub>2</sub>As<sub>2</sub> are shown in Fig. 1. We find that the arsenide and antimonide phases are in fact very similar. Both are narrow band gap

semiconductors with moderately heavy bands. Transport calculations show that sufficiently high thermopowers for waste heat recovery can be achieved in both materials at modest doping levels comparable to those in other semiconductor thermoelectric materials. However, in our magnetic calculations we find the material to be a local moment antiferromagnet, with very strong exchange interactions and strong spin dependent hybridization. This situation is particularly detrimental to the carrier mobility. The implication is that these materials are not likely to be useful thermoelectrics without strong modification. One possibility is to go to the Fe phase,  $\text{BaFe}_2\text{As}_2$  and alloy with Mn in order to obtain resonant scattering in analogy with TI-doped PbTe. However, considering that antimonide,  $\text{BaFe}_2\text{Sb}_2$  is not a known phase, and the acceptance of an arsenic based material in vehicular applications is unclear, we intend to pursue other materials in the coming quarter. A technical report will be submitted for publication describing these results in FY09-Q2.

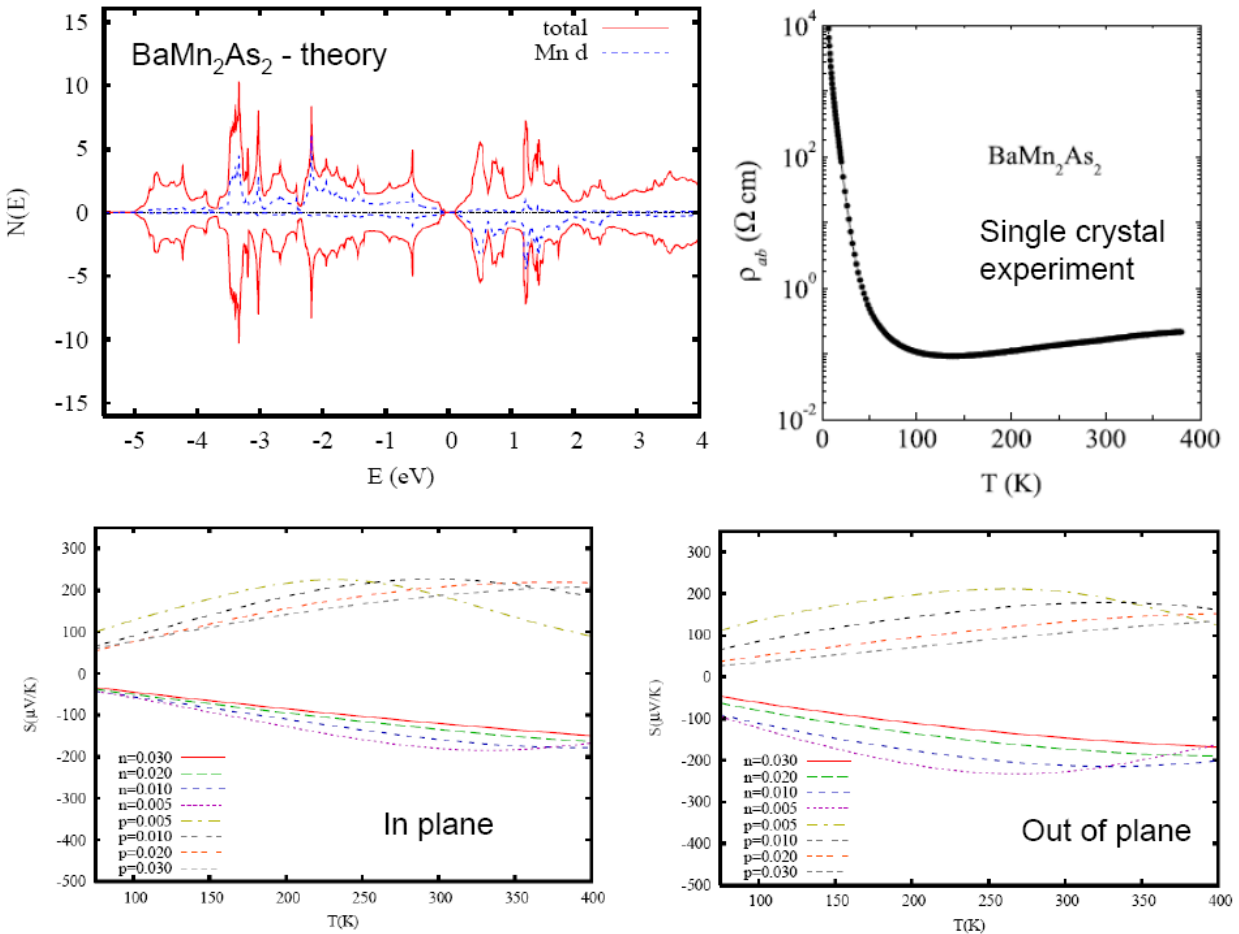


**Fig 1:** Calculated and experimental properties of  $\text{ThCr}_2\text{Si}_2$  structure  $\text{BaMn}_2\text{As}_2$ . (a – top left) calculated density of states showing narrow band gap semiconducting behavior; (b- top right) measured single crystal resistivity confirming semiconducting behavior. (c,d – bottom) Calculated in plane and out of plane thermoelectric power as a function of doping and temperature. Note that high values of the thermopower are obtained for low doping levels.

During FY08 we performed a series of electronic structure calculations, and identified delafossite structure  $YCuO_{2+x}$  with appropriate oxygen stoichiometry as a potential thermoelectric for vehicular applications. This material has nearly isotropic thermoelectric properties in contrast to other high ZT oxides (e.g.  $Na_xCoO_2$ ) and in addition is composed of inexpensive elements. During the current quarter we have continued investigation of this phase and have had ongoing interactions with C. Narula (ORNL) who has successfully synthesized the material. When thermoelectric characterization is done, it will be necessary to correlate the measured properties with the oxygen stoichiometry, which is variable in this phase. Calculations of doping dependent transport parameters will be very helpful for this. This will allow optimization of the thermoelectric performance. We will use our existing results and new calculations as needed to do this.

We also continued our collaboration with CalTech on cubic  $La_3Te_4$ . This material is a very high performance material at high temperature. Our primary focus has been to establish the doping level dependence, which may then be used to optimize the material at lower temperature for waste heat recovery. We found that there are two bands involved in transport, a moderate mass band for low carrier concentration followed by a heavy band onset at higher energy. During this quarter we completed analysis of the results and prepared a technical report for publication later in FY09. Although the two band character yields a weaker doping level dependence of the thermopower than a single band case, it is favorable for high mobility at low carrier density. As such, and especially considering the high performance of this material, further investigation seems warranted.

#### **Status of FY 2009 Milestones**

We are progressing towards our milestone of predicting a new thermoelectric composition. Strategies that will be used are to continue investigation of Cu containing delafossites, other narrow band oxide materials, and chalcogenides. Depending on the results we will continue with those materials and/or investigate alternate narrow band oxides containing mixed-valent transition element ions.

#### **Communications/Visits/Travel**

D.J. Singh: Travel to DTEC Meeting, Monterey California for presentation.

#### **Problems Encountered**

No significant problems encountered this quarter.

#### **Publications/Presentations/Awards**

##### **Presentations**

D.J. Singh, "Progress in the theory of thermoelectric materials", DTEC Meeting, Monterey, California.

##### **Awards**

D.J. Singh, ORNL Directors Award for Outstanding Individual Achievement in Science and Technology.

D.J. Singh, elected to the Publication Oversight Committee of the American Physical Society (Singh is a Fellow of the American Physical Society).

### **Publications**

J. An, A. Subedi and D.J. Singh, "Ab initio phonon dispersions of PbTe", *Solid State Communications* **148**, 417 (2008).

### **References**

1. D.J. Singh and L. Nordstrom, *Planewaves, Pseudopotentials and the LAPW Method, 2<sup>nd</sup> Edition*, Springer, Berlin, 2006.
2. G.K.H. Madsen and D.J. Singh, "BoltzTraP: A code for calculating band-structure dependent quantities", *Computer Physics Commun.* **175**, 67 (2006).